

Article

Survival and Genome Evolution Signatures of *Klebsiella pneumoniae* Isolates Originated in Seven Species of Aquatic Animals

Huiqiong Guan^{1,2}, Lu Xie³  and Lanming Chen^{1,2,*}

¹ Key Laboratory of Quality and Safety Risk Assessment for Aquatic Products on Storage and Preservation (Shanghai), Ministry of Agriculture and Rural Affairs of the People's Republic of China, Shanghai 201306, China

² College of Food Science and Technology, Shanghai Ocean University, Shanghai 201306, China

³ Shanghai-MOST Key Laboratory of Health and Disease Genomics, Institute for Genome and Bioinformatics, Shanghai Institute for Biomedical and Pharmaceutical Technologies, Shanghai 200032, China

* Correspondence: lmchen@shou.edu.cn

Abstract: *Klebsiella pneumoniae* can cause life-threatening pneumonia in humans. The bacterium is also the causative agent of nosocomial infection diseases. In our recent research, we reported, for the first time, the presence of *K. pneumoniae* in fourteen species of aquatic animals sampled in Shanghai, China. Here, we further investigated the bacterial survival and genome evolution traits. The results revealed that *K. pneumoniae* isolates ($n = 7$), recovered from 7 species of commonly consumed aquatic animals, had multiple antibiotic and heavy metal resistance profiles. The isolates were capable of growing vigorously at pH 4.5–7.5 and 0.5–1.0% NaCl in TSB medium at 37 °C. Draft genome sequences of the *K. pneumoniae* isolates were determined (5,256,522–5,857,823 bp, 56.35–57.81% GC contents), which carried many mobile genetic elements, including genomic islands ($n = 87$), prophages ($n = 14$), integrons ($n = 4$), and insertion sequences ($n = 22$), indicating possible active horizontal gene transfer during the genome evolution. Meanwhile, numerous strain-specific ($n = 199$ –605) genes, antibiotic resistance ($n = 20$ –35, e.g., β -lactamase) genes, and virulence ($n = 43$ –59, e.g., enterobactin)-related genes, were also identified, demonstrating considerable genome variation in the *K. pneumoniae* isolates. Overall, the results of this study fill prior gaps in understanding the *K. pneumoniae* genomes derived from aquatic animals.

Keywords: *Klebsiella pneumoniae*; aquatic animal; genome; mobile genetic element; virulence; antibiotic resistance; heavy metal resistance



Citation: Guan, H.; Xie, L.; Chen, L. Survival and Genome Evolution Signatures of *Klebsiella pneumoniae* Isolates Originated in Seven Species of Aquatic Animals. *Diversity* **2023**, *15*, 527. <https://doi.org/10.3390/d15040527>

Academic Editors: Naoko Takezaki and Ben-Yang Liao

Received: 25 January 2023

Revised: 31 March 2023

Accepted: 2 April 2023

Published: 6 April 2023



Copyright: © 2023 by the authors. Licensee MDPI, Basel, Switzerland. This article is an open access article distributed under the terms and conditions of the Creative Commons Attribution (CC BY) license (<https://creativecommons.org/licenses/by/4.0/>).

1. Introduction

Klebsiella pneumoniae was first described by Carl Friedlander in 1882, which was isolated from the lungs of patients who died from pneumonia [1]. Since then, the Gram-negative bacterium has also been reported to cause bloodstream infections (BSIs), meningitis, osteomyelitis, thrombophlebitis, urinary tract infections (UTIs), and invasive pyogenic liver abscess syndrome [2–4]. To date, more than 79 capsular (K antigen) serotypes have been reported in *K. pneumoniae* isolates, of which K1, K2, K5, K20, K54, and K57 serotypes are strongly associated with the bacterial pathogenesis [5,6].

Antibiotics are widely used in clinics for prevention and therapy of bacterial infections [3]. Nevertheless, the overuse and/or misuse of antibiotics have accelerated the spread of antibiotic-resistant pathogens, particularly in developing countries [2,7,8]. For instance, in China, more than 40% (267/666) of clinical *K. pneumoniae* isolates, collected from 30 medical centers across the country, were identified as carbapenem-resistant *K. pneumoniae* (CRKP) in 2017 [7]. The mortality of patients with CRKP infection (main BSIs) was up to 70% [8]. The rising incidence of multiple drug resistant (MDR) *K. pneumoniae* creates serious threats to public health.

K. pneumoniae are found growing in hospital wastewaters, urban rivers, and even in shrimp farms [9–12]. Intensive farming in aquaculture drives indiscriminate use of antibiotics, which results in antibiotic residues in aquatic products and MDR pathogens [13]. For example, recently, Luo et al. [14] detected chloramphenicol (CHL) residue in shrimp, shellfish, and fish samples ($n = 291$) sampled in Shenzhen, China. They found that positive detection rates of CHL were 13.6% (3/22), 37.2% (64/172), and 16.5% (16/97) in shrimp, shellfish, and fish, respectively [14]. Xu et al. [15] recently reported *K. pneumoniae* isolates ($n = 94$) present in 14 species of aquatic animals sampled in Shanghai, China, which showed higher resistance rates to sulfamethoxazole–trimethoprim (SXT, 52.1%) and CHL (31.9%). On the other hand, heavy metal concentrations in marine environments, rivers, and soils have been increasing because of industrialization and environmental pollution, which has given rise to heavy-metal-tolerant bacteria [16]. Moreover, heavy metals could trigger the proliferation of antibiotic resistance by increasing mobile genetic element (MGE) abundance or by influencing bacterial communities [17]. It has been reported that the majority of the *K. pneumoniae* isolates were also tolerant to heavy metals e.g., Cr^{3+} (96.8%), Pb^{2+} (89.4%), and Hg^{2+} (81.9%) [15]. The co-selection between antibiotics and heavy metals, leading to MDR *K. pneumoniae*, threatens population health [18,19].

Aquatic environments, considered as a pool of antibiotic resistance genes (ARGs), contain diverse microbial communities, where the dissemination of ARGs could partially be attributed to horizontal gene transfer (HGT) mediated via MGEs in bacterial genomes [20,21]. To date, complete genome sequences of over 1757 *K. pneumoniae* isolates are available in the GenBank database (<https://www.ncbi.nlm.nih.gov/>, accessed on 14 March 2023). Of these, the majority of the *K. pneumoniae* strains ($n = 1659$) were isolated from humans, followed by animals ($n = 87$), water environments ($n = 4$), and others ($n = 7$). To the best of our knowledge, current literature on the genomes of *K. pneumoniae* isolates originating in aquatic animals is rare.

In our recent research, we reported, for the first time, the presence of *K. pneumoniae* in 14 species of aquatic animals [15]. Based on the finding, in this study, we further investigated the survival and genome evolution traits of the *K. pneumoniae* isolates recovered from seven species of commonly consumed aquatic animals. The major objectives of this study were (1) to examine phenotypes, genotypes, and growth traits of the *K. pneumoniae* isolates; (2) to determine draft genome sequences of the *K. pneumoniae* isolates using the Illumina HiSeq \times Ten sequencing technique and to identify MGEs, such as genomic islands (GIs), prophages, integrons (INs), and insertion sequences (ISs) in the *K. pneumoniae* genomes; (3) to identify virulence- and resistance-related genes in the *K. pneumoniae* genomes; and (4) to analyze phylogenetic relatedness of the *K. pneumoniae* isolates. The results of this study will enrich genome data and fill prior gaps in understanding *K. pneumoniae* genomes derived from aquatic animals.

2. Materials and Methods

2.1. *K. pneumoniae* Isolates and Cultural Conditions

K. pneumoniae strains (Table S1) were isolated from three species of shellfish: *Maotracia veneriformis*, *Cipangopaludina cahayensis* and *Tegillarca granosa*; two species of crustaceans: *Eriocheir sinensis* and *Procambarus clarkii*; and two species of fish: *Epinephelus fuscoguttatus* and *Misgurnus anguillicaudatus*, which were sampled in Shanghai, China in July–September of 2018–2019 [15]. The *K. pneumoniae* isolates were identified by biochemical and molecular biological methods [15] and stored at $-80\text{ }^{\circ}\text{C}$ in a freezer in our laboratory at Shanghai Ocean University, in Shanghai, China. The isolates were routinely incubated in Tryptic Soy Broth (TSB) medium (pH 7.2, 0.5% NaCl) (Beijing Land Bridge Technology, Beijing, China) at $37\text{ }^{\circ}\text{C}$ aerobically, with shaking at 175 rpm [15]. *K. pneumoniae* ATCC13883 was used as a positive control strain.

2.2. Antibiotic Susceptibility and Heavy Metal Tolerance Assays

Antibiotic susceptibility of the *K. pneumoniae* isolates were tested according to the disc diffusion method approved by the Clinical and Laboratory Standards Institute in the United State (CLSI, M100-S28, 2018). The Mueller–Hinton (MH) medium and antibiotic discs were purchased from OXOID, Basingstoke, UK, as described in our recent reports [15,22]. Heavy metal tolerance of the *K. pneumoniae* isolates was performed according to the broth dilution testing (microdilution, CLSI) [15,22]. The HgCl₂, NiCl₂, CrCl₃, CdCl₂, PbCl₂, CuCl₂, ZnCl₂, and MnCl₂ (Analytical Reagent, Sinopharm Chemical Reagent Co., Ltd., Shanghai, China) were applied in the range from 3200 to 3.125 µg/mL. The results were interpreted by minimal inhibitory concentrations (MICs) that completely inhibited the growth of the bacteria. *Escherichia coli* ATCC25922 and K12 strains (Institute of Industrial Microbiology, Shanghai, China) were used as quality control strains [15,22].

2.3. Growth Curve Assay

The TSB was adjusted to different pH (3.5, 4.5, 5.5, 6.5, and 7.5) and NaCl concentrations (0.5%, 1%, 2%, 3%, and 4%) as described in our previous studies [23,24]. Growth curves of the *K. pneumoniae* isolates under different pH (3.5–7.5) and NaCl (0.5–4%) conditions were individually determined at 37 °C for 25 h using Multimode Microplate Reader (BioTek Instruments, Winooski, VT, USA).

2.4. Polymerase Chain Reaction (PCR) Assay

The 16S rRNA gene, virulence-associated genes (*aerobactin*, *magA*, *tarT*, *wcaG*, *iroN*, *rmpA*, *entB*, *fimH*, *mrkD*, and *ybtA*), and capsule serotypes (K1, K2, K5, K20, K54, and K57) were detected using the PCR assay as described in our recent report [15]. The primers (Table S2) were synthesized by the Sangon (Shanghai, China).

2.5. Genome Sequencing, Assembly, and Annotation

The *K. pneumoniae* isolates were individually incubated in the TSB (pH 7.2, 0.5% NaCl) to logarithmic growth stage (LGS). Bacterial cells were harvested by centrifugation, and genomic DNA was extracted using TIANamp Bacteria DNA Kit (Tiagen Biochemical Technology Co., Ltd., Beijing, China) according to the manufacture's instruction. Three separately produced DNA samples were used for each of the *K. pneumoniae* isolates. DNA samples were analyzed, as described in our previous report [21,24], and only high quality samples were subjected to the genome sequencing.

Whole-genome sequencing of the *K. pneumoniae* isolates was conducted by Shanghai Majorbio Bio-Pharm Technology Co., Ltd., Shanghai, China, using Illumina HiSeq × Ten (Illumina, San Diego, CA, USA) platform [21]. High-quality sequence assembly was performed using SOAPdenovo (version 2.04) software [25]. Coding sequences (CDSs), rRNA genes, tRNA genes, and Clusters of Orthologous Groups (COG) of proteins were predicted using the same software Glimmer (version 3.02) [26], Barrnap tool (<https://github.com/tseemann/barrnap>, accessed on 31 July 2022), tRNAscan-SE (version 2.0) [27], and Basic Local Alignment Search Tool (BLAST, <http://www.ncbi.nlm.nih.gov/BLAST>, accessed on 31 July 2022) with default parameters as described in our recent report [18]. The virulence factor database (<http://www.mgc.ac.cn/VFs>, accessed on 31 July 2022) and the ARGs database (<http://arpcard.Mcmaster.ca>, accessed on 31 July 2022) were used to detect virulence- and antibiotic resistance-related genes, respectively [18].

2.6. Comparative Genome Analysis

GIs, prophages, INs, ISs, and CRISPR-Cas repeats in the *K. pneumoniae* genomes were predicted using the same software IslandViewer (version 1.2) [28], Phage_Finder [29], Integron_Finder (version 2.0) [30], ISEScan (version 1.7.2.1) [31], as well as Mined software (version 3) and CRISPRtyper [32] with default parameters as described in our recent report [21].

Core genes were the set of genes encoding orthologous proteins in all the genomes tested, while pan-genes were the set of all genes present in all the tested genomes. Only proteins with $\geq 60\%$ amino acid similarity and $\geq 80\%$ sequence coverage were designated as direct relatives, while those with $\leq 30\%$ or no hits were assigned as strain-specific genes at $E \leq 1 \times 10^{-5}$ [21].

A phylogenetic tree was constructed on the basis of amino acid data sets of single-copy orthologs that were present in all the analyzed genomes of 72 *K. pneumoniae* isolates, of which complete genome sequences of 65 *K. pneumoniae* isolates were downloaded from the GenBank database (Table S3). The maximum likelihood method was used to build a tree by RAxML (version 8) software [33], with 1000 bootstrap replications and a cut-off threshold of $\geq 50\%$ bootstrap values.

2.7. Statistical Analysis

The SPSS statistical analysis software (version 17.0, SPSS Inc., Chicago, IL, USA) was used to analyze the data. All tests were conducted in triplicate.

3. Results

3.1. Phenotypes and Genotypes of the *K. pneumoniae* Isolates

K. pneumoniae 7-5-4, 7-10-14, 7-13-2, 7-17-8, 8-1-12-1, 8-2-5-4, and 8-2-10-5 strains (Table S1) were isolated from 7 species of aquatic animals, including *M. anguillicaudatus*, *M. veneriformis*, *E. sinensis*, *C. cahayensis*, *P. clarkii*, *T. granosa*, and *E. fuscoguttatus*, respectively [15]. The isolates were confirmed by 16S rRNA gene sequencing and analysis, and the obtained 16S rDNA sequences were deposited in the National Center for Biotechnology Information (NCBI) database under the accession numbers shown in Table S1.

The *K. pneumoniae* isolates had different antibiotic resistance profiles (Table S1). For example, *K. pneumoniae* 7-5-4 from *M. anguillicaudatus* displayed resistance to CHL, ciprofloxacin (CIP), kanamycin (KAN), norfloxacin (NOR), SXT, and tetracycline (TET), while *K. pneumoniae* 7-10-14 from *M. veneriformis* was resistant to ampicillin (AMP), CHL, gentamicin (GEN), KAN, SXT, and TET. Conversely, *K. pneumoniae* 7-13-2, 7-17-8, and 8-1-12-1 isolates were solely resistant to AMP.

Meanwhile, the *K. pneumoniae* isolates tolerated 3–7 heavy metals, showing different tolerance patterns. For example, *K. pneumoniae* 8-1-12-1 from *P. clarkii* was tolerant to $Zn^{2+}/Pb^{2+}/Mn^{2+}/Hg^{2+}/Cu^{2+}/Cr^{3+}/Cd^{2+}$, while *K. pneumoniae* 8-2-10-5 from *E. fuscoguttatus* was tolerant to $Zn^{2+}/Pb^{2+}/Hg^{2+}/Cu^{2+}/Cr^{3+}/Cd^{2+}$. Conversely, *K. pneumoniae* 7-17-8 from *C. cahayensis* tolerated the minimum number of heavy metals ($Zn^{2+}/Cu^{2+}/Cr^{3+}$) tested.

In addition, all the *K. pneumoniae* isolates tested negative for the virulence-related genes, including the *aerobactin*, *magA*, *tarT*, *wcaG*, *iroN*, and *rmpA*. However, some virulence-related genes tested positive in the *K. pneumoniae* isolates. For instance, *K. pneumoniae* 7-10-14 carried the *entB* gene; *K. pneumoniae* 7-5-4, 7-13-2, 8-2-5-4, and 8-2-10-5 isolates tested positive for the *entB/fimH/mrkD* genes; and *K. pneumoniae* 7-17-8, and 8-1-12-1 isolates had the *entB/fimH/mrkD/ybtA* gene profile.

3.2. Survival of the *K. pneumoniae* Isolates at Different pH and NaCl Conditions

The pH of the human stomach normally ranges pH 1–3, but can rise above 6.0 after food consumption [23]. Therefore, we examined survival of the *K. pneumoniae* isolates at different pH conditions (pH 3.5–7.5) when incubated in the TSB (0.5% NaCl) at 37 °C. As shown in Figure 1A–G, the growth of all *K. pneumoniae* isolates was severely inhibited at the acidic pH 3.5. However, notably, the acidic pH 4.5 condition strongly promoted the bacterial growth, and all the isolates were capable of growing vigorously at pH 4.5–7.5. The highest biomass was observed at pH 7.5, with the maximum OD_{600} at stationary growth phase (SGP) in the range of 1.37–1.51 (Figure 1).

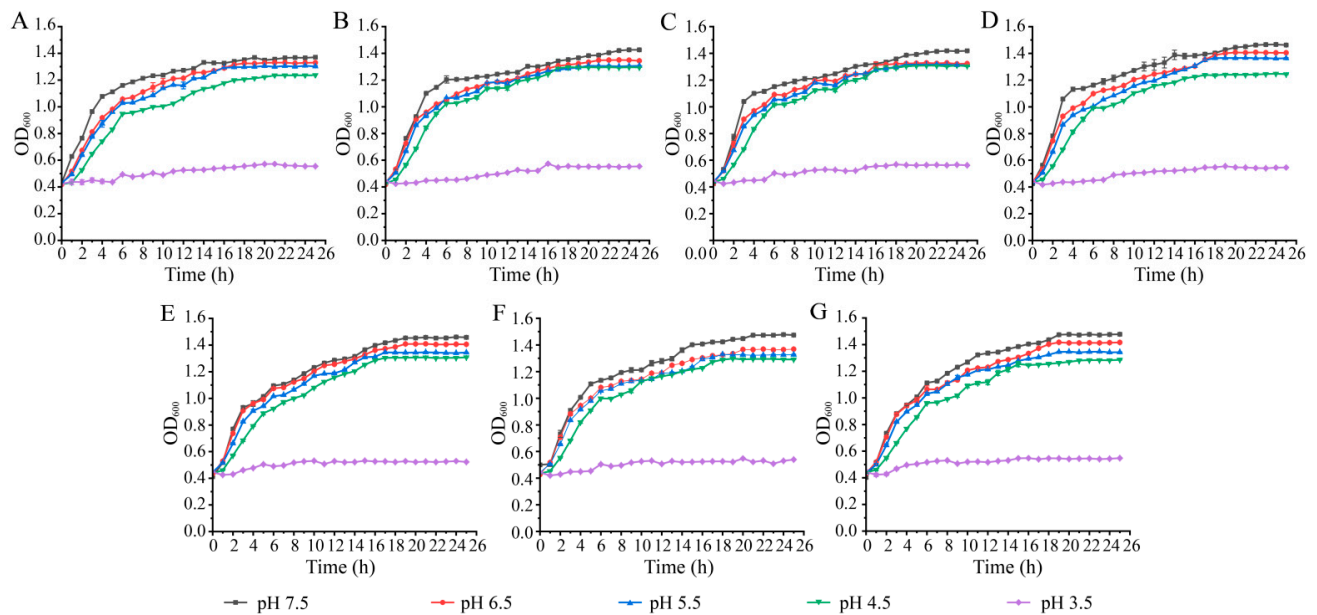


Figure 1. Growth of the *K. pneumoniae* isolates under different pH conditions. The isolates were incubated in the TSB (0.5% NaCl) at 37 °C. (A–G): *K. pneumoniae* 7-5-4, 7-10-14, 7-13-2, 7-17-8, 8-1-12-1, 8-2-5-4, and 8-2-10-5, respectively.

Given that the *K. pneumoniae* isolates were recovered from different aquatic animals in water environments, we further determined growth curves of the *K. pneumoniae* isolates at different salinity concentrations (0.5–4% NaCl) when incubated in the TSB (pH 7.5) at 37 °C. As shown in Figure 2A–G, the growth of all *K. pneumoniae* isolates was severely inhibited at 4% NaCl. The biomass of the *K. pneumoniae* isolates gradually increased with the decreased NaCl concentrations (3–0.5%), and the highest biomass was observed at 0.5% NaCl, showing the maximum OD₆₀₀ values ranging from 1.26 to 1.44 at SGP.

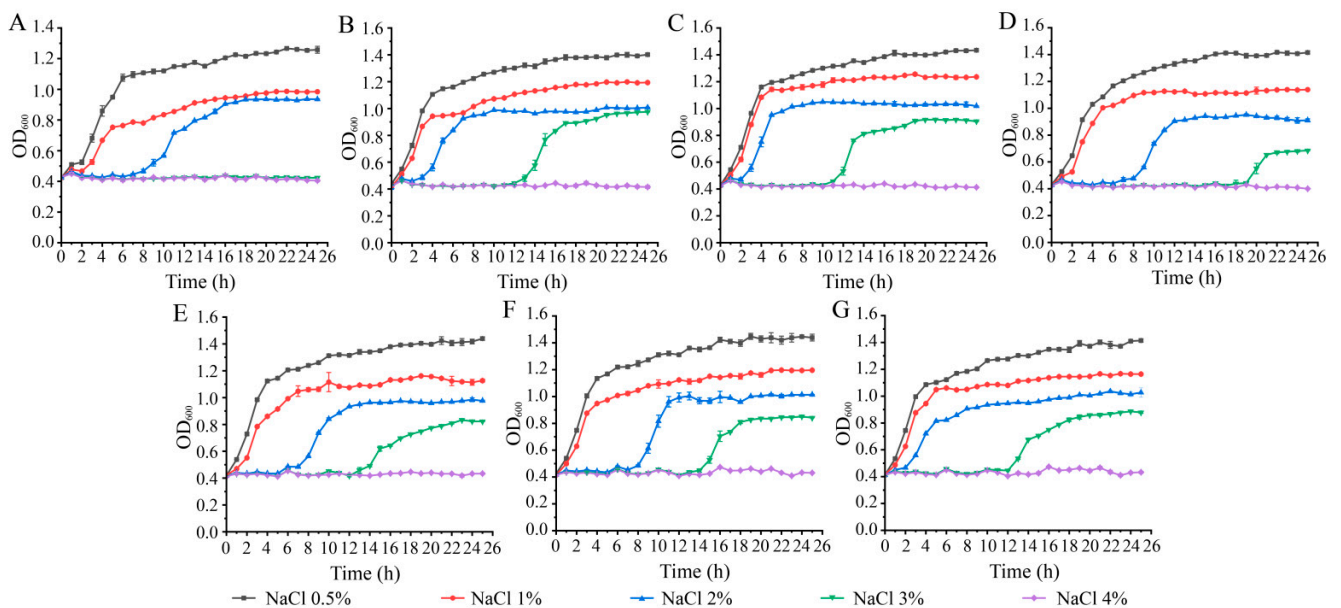


Figure 2. Growth of the *K. pneumoniae* isolates under different concentrations of NaCl. The isolates were incubated in the TSB (pH 7.5) at 37 °C. (A–G): *K. pneumoniae* 7-5-4, 7-10-14, 7-13-2, 7-17-8, 8-1-12-1, 8-2-5-4, and 8-2-10-5, respectively.

For example, *K. pneumoniae* 7-5-4 from *M. anguillicaudatus* appeared the most susceptible to the higher salinity concentrations, as this isolate was strongly repressed at 3% NaCl as well. Conversely, this condition stimulated the growth of the other 6 isolates, but showed a longer retarded growth phase (RGP) (11–19 h) with lower biomass ($OD_{600} = 0.68–0.97$). The decreased NaCl concentration (2%) promoted the growth of *K. pneumoniae* 7-5-4, although it had an RGP for 8 h. *K. pneumoniae* 7-5-4 was able to grow vigorously at 1.0–0.5%, the same case as the other isolates.

Taken together, the results demonstrated that the *K. pneumoniae* isolates of aquatic animal origins were able to grow vigorously at pH 4.5–7.5, 0.5–1.0% NaCl in the TSB at 37 °C. *K. pneumoniae* 7-5-4 was the most susceptible to higher salinity concentrations (4–3 NaCl) among the isolates tested in this study.

3.3. Genome Features of the *K. pneumoniae* Isolates of Aquatic Animal Origins

Based on the obtained results, we further determined draft genome sequences of the 7 *K. pneumoniae* isolates using the Illumina HiSeq × Ten sequencing platform, which generated approximately 76,382–107,851 clean single reads. The final assembly yielded 45–113 scaffolds with sequencing depth (on average) of 188.3-fold to 271.9-fold. The obtained genome sizes ranged from 5,256,522 to 5,857,823 bp with GC contents of 56.35–57.81% (Table 1, Figure S2). A total of 4885–5558 protein-coding genes were predicted, of which approximately 4639–4986 genes were classified into 22 functional catalogs in the COG database. Remarkably, the *K. pneumoniae* genomes carried many MGEs, including GIs ($n = 87$), prophages ($n = 14$), INs ($n = 4$), and ISs ($n = 22$), suggesting the HGT during the *K. pneumoniae* genome evolution via these MGEs.

Table 1. Genome features of the *K. pneumoniae* isolates of aquatic animal origins.

Genome Feature	<i>K. pneumoniae</i> Isolate						
	7-5-4	7-10-14	7-13-2	7-17-8	8-1-12-1	8-2-5-4	8-2-10-5
Genome size (bp)	5,857,823	5,376,532	5,412,275	5,438,640	5,593,530	5,432,731	5,256,522
G + C (%)	56.35	57.28	57.29	57.12	57.21	57.32	57.81
DNA Scaffold	81	113	79	50	74	64	45
Total predicted gene	5662	5142	5165	5189	5369	5143	4986
Protein-coding gene	5558	5044	5060	5089	5260	5042	4885
RNA gene	240	231	238	234	249	224	235
Genes assigned to COG	4986	4761	4757	4770	4916	4777	4639
Genes with unknown function	1363	1230	1288	1271	1357	1230	1188
GI	17	8	8	15	16	11	12
Prophage	2	2	2	2	3	1	2
IN	1	2	0	0	0	0	1
IS	2	2	6	2	4	4	2
CRISPR-Cas repeat	14	9	6	2	6	6	11
Source	This study	This study	This study	This study	This study	[15]	This study

The draft genomes of the *K. pneumoniae* 7-5-4, 7-10-14, 7-13-2, 7-17-8, 8-1-12-1, 8-2-5-4 and 8-2-10-5 isolates were deposited in the GenBank database under the accession numbers JALJQY000000000, JALJQX000000000, JALJQW000000000, JALJQV000000000, JALJQT000000000, JALJQQ000000000, and JALJQR000000000, respectively.

3.4. MGEs in the *K. pneumoniae* Genomes of Aquatic Animal Origins

3.4.1. GIs

GIs can carry large foreign DNA fragments (~200 Kb) and endorse the host's diverse biological functions [21]. In this study, remarkably, a total of 87 GIs were identified in the 7 *K. pneumoniae* genomes (Table S4), each of which contained 8–17 GIs, ranging from 3228 to 44,595 bp and encoding 5–47 genes (Figure 3). Interestingly, various functions

carried by the GIs were found, e.g., virulence, resistance, substrate hydrolysis, transporting and utilization, restriction and modification, as well as phage and stress regulation.



Figure 3. Cont.

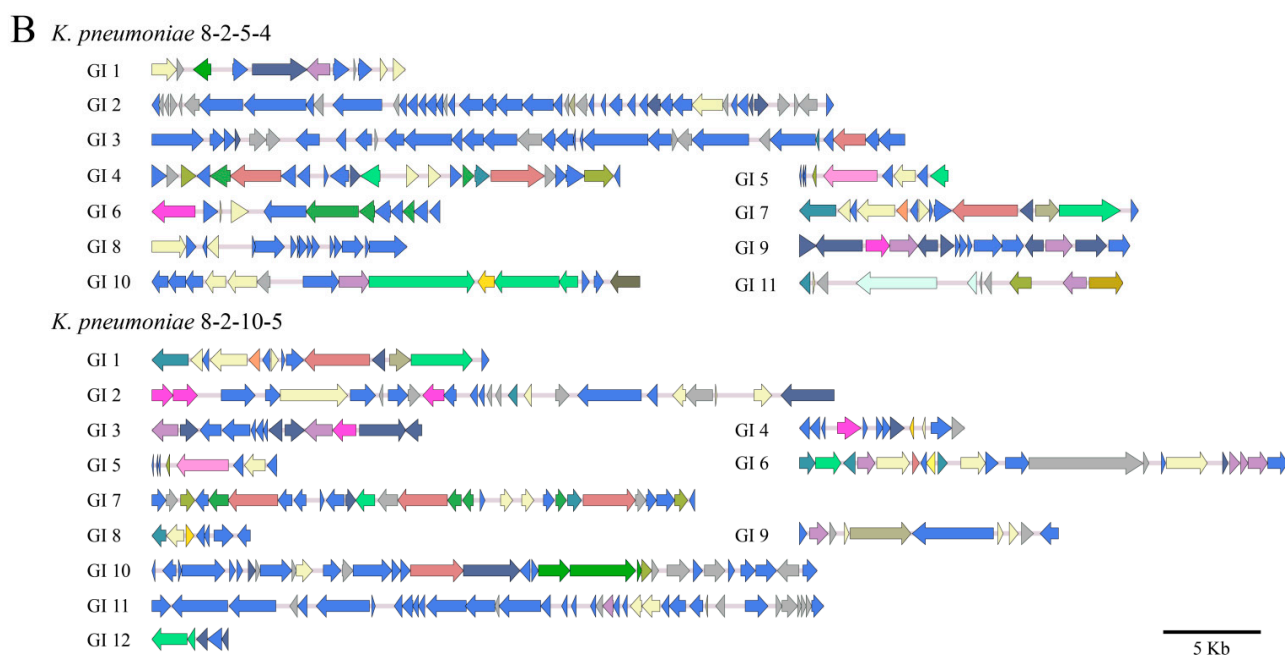


Figure 3. Gene organizations of the GIs identified in the *K. pneumoniae* genomes (A,B). Different colors referred to COG classification to mark gene functions, and genes not annotated to COG database were displayed in grey.

The *K. pneumoniae* 7-5-4 genome contained the maximum number of the GIs ($n = 17$, GIs 1–17), whereas *K. pneumoniae* 7-10-14 had the fewest GIs ($n = 8$, GIs 1–8). Of note, virulence-related genes were found in 10 GIs in the 7 *K. pneumoniae* genomes (Table S5). For example, the *hcp* gene was present in the GI 12, GI 1, GI 3, GI 16, and GI 3 in *K. pneumoniae* 7-5-4, 7-10-14, 7-17-8, 8-1-12-1, and 8-2-5-4 genomes, respectively. It is a core gene of the T6SS in *Acinetobacter baumannii*, causing respiratory tract infection [34]. Antibiotic resistance and heavy-metal-tolerance-related genes were identified in some GIs, e.g., the GI 3 (17,350 bp) and GI 8 (6626 bp) in the *K. pneumoniae* 7-13-2 genome, respectively. Interestingly, the conjugative transfer-related genes were found in the GI 11 in *K. pneumoniae* 7-17-8. Additionally, there were some identified GIs carrying phage regulator genes in the *K. pneumoniae* genomes. For example, the GI 5 in *K. pneumoniae* 7-5-4, and the GI 11 in *K. pneumoniae* 8-1-12-1 contained the gene (*Kp* 7-5-4_1988; *Kp* 8-1-12-1_3134) encoding a lysB family phage lysis regulatory protein.

3.4.2. Prophages

Prophages are viruses that infect bacteria. They can transfer important biological characteristics to their bacterial hosts [35]. In this study, a total of 14 prophage gene clusters were identified in the 7 *K. pneumoniae* genomes (Table S6), each of which carried 1–3 prophages, ranging from 21,338 to 108,967 bp and encoding 34–115 genes (Figure 4).

The *K. pneumoniae* 8-1-12-1 genome contained the maximum number of prophage gene clusters ($n = 3$), which had sequence similarity to *Ralstonia*_phage_RSA1 (38,760 bp, NCBI accession number: NC_009382), *Enterobacteria*_phage_186 (30,624 bp, NCBI accession number: NC_001317), and *Klebsiella*_phage_phiKO2 (51,601 bp, NCBI accession number: NC_005857). Conversely, *K. pneumoniae* 8-2-5-4 carried only 1 prophage gene cluster similar to *Enterobacteria*_phage_HK022 (15,456 bp, NCBI accession number: NC_002161).

The identified 14 prophages in the 7 *K. pneumoniae* genomes were derived from 4 different genera, including *Enterobacteria*, *Klebsiella*, *Pseudomonas*, and *Ralstonia*, indicating extensive phage transmission across the genera boundaries. Moreover, the *Enterobacteria*_phage_186 homologue was present in the *K. pneumoniae* 7-5-4 and 8-1-12-1 genomes, but in different lengths, encoding different numbers of genes. The same was the case for

the *Pseudomonas*_phage_D3 homologue, which was present in the *K. pneumoniae* 7-5-4 and 7-10-14 genomes. Likewise, the *Klebsiella*_phage_phiKO2 homologue was found in the *K. pneumoniae* 7-17-8, 8-1-12-1 and 8-2-10-5 genomes carrying a similar set of phage structure genes but different accessory genes. These results also provided evidence of extensive genome rearrangement during the *K. pneumoniae* genome evolution.

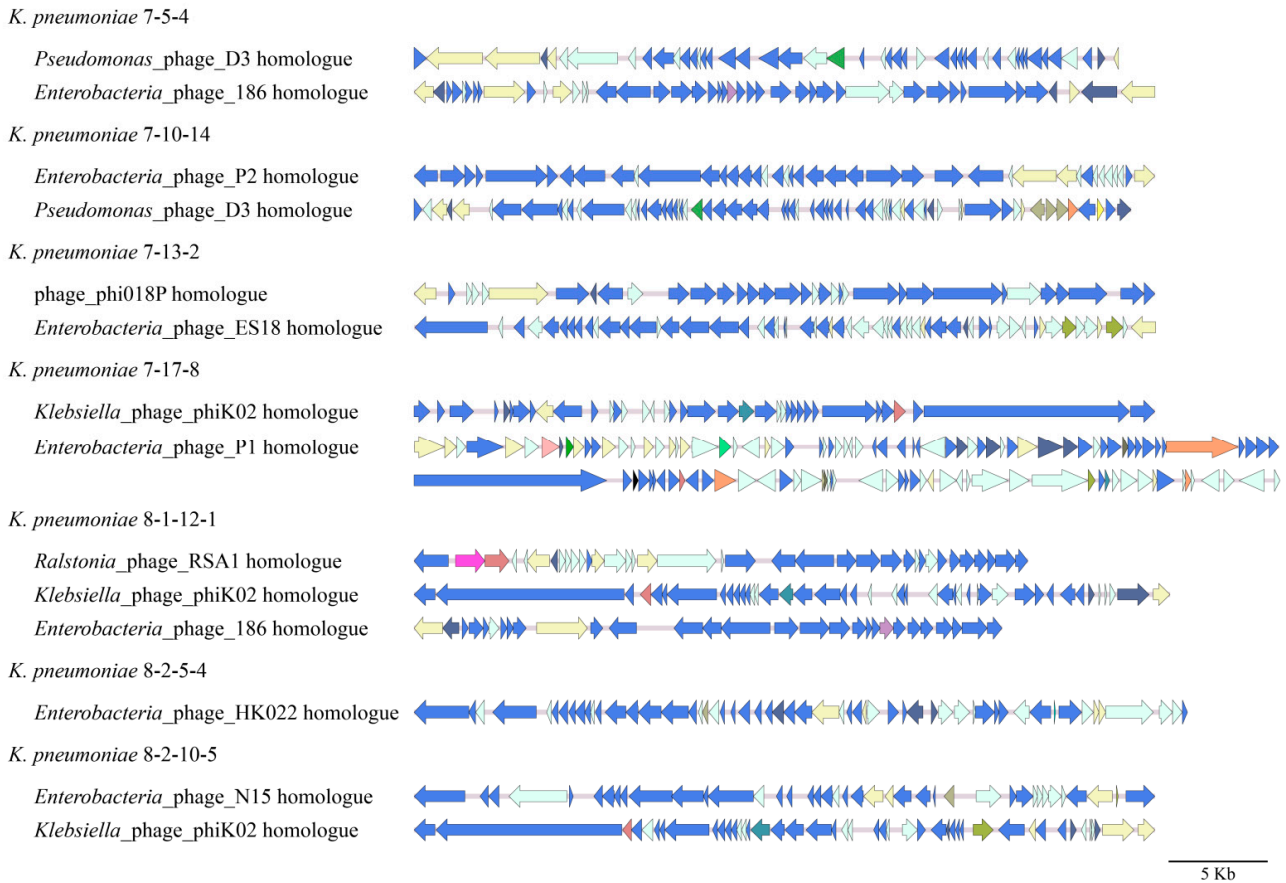


Figure 4. Gene organizations of the prophages identified in the *K. pneumoniae* genomes.

3.4.3. INs

INs are considered as determinants in acquisition and evolution of virulence and antibiotic resistance [36]. They are classified into type I, type II, type III, and super integrons based on integrase genes (*intI1*, *intI2*, *intI3*, and *intI4*) [21]. In this study, INs were identified in the *K. pneumoniae* 7-5-4 ($n = 1$), 7-10-14 ($n = 2$), and 8-2-10-5 ($n = 1$) genomes, but absent from *K. pneumoniae* 7-13-2, 7-17-8, 8-1-12-1, and 8-2-5-4 genomes (Figure 5, Table S7).

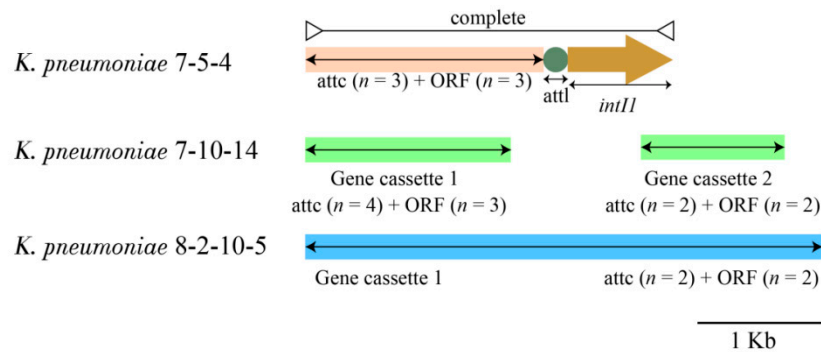


Figure 5. The structure diagram of the INs identified in the *K. pneumoniae* genomes.

The *K. pneumoniae* 7-5-4 genome contained only 1 complete IN (2737 bp), encoding a NAD (+)-rifampin ADP-ribosyltransferase Arr-2 (Kp 7_5_4_5567), an ANT(3'')-Ia family aminoglycoside nucleotidyltransferase AadA3 (Kp 7_5_4_5566), an Orf3/QacEdelta1 fusion protein (Kp 7_5_4_5565), and an *int11* (Kp 7_5_4_5568). The type 1 INs are strongly associated with the dissemination of antibiotic resistance in bacteria [37].

The *K. pneumoniae* 7-10-14 genome contained 2 incomplete INs (INs 1–2) with gene cassettes. The IN 1 encoded an aac(6')-Ib family aminoglycoside 6'-N-acetyltransferase (Kp 7_10_14_5082), a NAD(+)-rifampin ADP-ribosyltransferase (Kp 7_10_14_5083), and a dihydrofolate reductase type 15 (Kp 7_10_14_5084), while the IN 2 encoded a quaternary ammonium compound efflux SMR (Kp 7_10_14_5103) and an aminoglycoside resistance protein (Kp 7_10_14_5104).

The *K. pneumoniae* 8-2-10-5 genome contained 1 incomplete IN, encoding a glycoside hydrolase family 31 protein (Kp 8_2_10_5_0283) and an ABC-F family ATPase (Kp 8_2_10_5_0284).

3.4.4. ISs

ISs are short discrete DNA fragments that can move themselves to a new position in DNA almost randomly in a single cell [38]. In this study, all the 7 *K. pneumoniae* genomes contained ISs ($n = 2$ to 6), ranging from 741 to 1588 bp (Table S8).

For instance, the *K. pneumoniae* 7-13-2 genome contained the maximum numbers of ISs ($n = 6$, IS001–IS006). The IS001 (807 bp) coded for a tyrosine-type recombinase/integrase (Kp 7_13_2_0367); IS002 (1265 bp) for a transposase IS116/IS110/IS902 family (Kp 7_13_2_4341); IS003 (1161 bp) for transposases (Kp 7_13_2_4675, Kp 7_13_2_4676); IS004 (1173 bp) for a IS5 family transposase (Kp 7_13_2_4820); IS005 (1257 bp) for a IS3 family transposase (Kp 7_13_2_5141, Kp 7_13_2_5142); and IS006 (819 bp) for a IS6-like element IS26 family transposase (Kp 7_13_2_5153).

3.5. CRISPR-Cas Repeats

The CRISPR-Cas systems provide adaptive immunity to prokaryotes from invasion by foreign nucleic acids in their hosts [39]. The systems are associated with drug resistance in *K. pneumoniae* [40,41]. In this study, a number of CRISPR-Cas repeats ($n = 54$) were identified in the 7 *K. pneumoniae* genomes, each of which contained 2–14 such gene clusters, ranging from 75 to 2649 bp. However, none of these systems contained the Cas protein, suggesting partial or inactive CRISPR-Cas systems in the *K. pneumoniae* isolates (Figure 6).

For instance, the *K. pneumoniae* 7-5-4 genome contained the maximum number of the CRISPR-Cas repeats ($n = 14$, CRISPRs 1–14), ranging from 77 to 2649 bp. The CRISPR 4 was the longest in size (2649 bp), with the maximum number of repetitive sequences ($n = 44$), whereas the CRISPR 3 was the shortest (77 bp), with the fewest repeats ($n = 2$). Conversely, the *K. pneumoniae* 7-17-8 genome had the fewest CRISPR-Cas repeats ($n = 2$, CRISPRs 1–2). The CRISPR 1 (201 bp) had 4 repeats, while the CRISPR 2 (188 bp) had 3 repeats.

3.6. Putative Virulence-Associated Genes in the *K. pneumoniae* Genomes

Many putative virulence-related genes ($n = 43–59$) were identified in the 7 *K. pneumoniae* genomes (Table 2). *K. pneumoniae* 8-1-12-1 form *P. clarkii* contained the maximum number of such genes ($n = 59$), whereas *K. pneumoniae* 7-10-14 from *M. veneriformis* carried relatively fewer ($n = 43$).

For instance, the *entABCDEFs* and *fepABCDG* gene clusters were identified in all the *K. pneumoniae* genomes, both of which are related to enterobactin in *K. pneumoniae*. The former is responsible for enterobactin biosynthesis, while the latter mediates enterobactin transport. Specifically, the *fepA* gene encodes a receptor for enterobactin uptake [3]. Of note, the *iucABCD* gene cluster was found in the *K. pneumoniae* 8-2-5-4 genome, which is involved in the biosynthesis of aerobactin, commonly detected in hypervirulent *K. pneumoniae* [42].

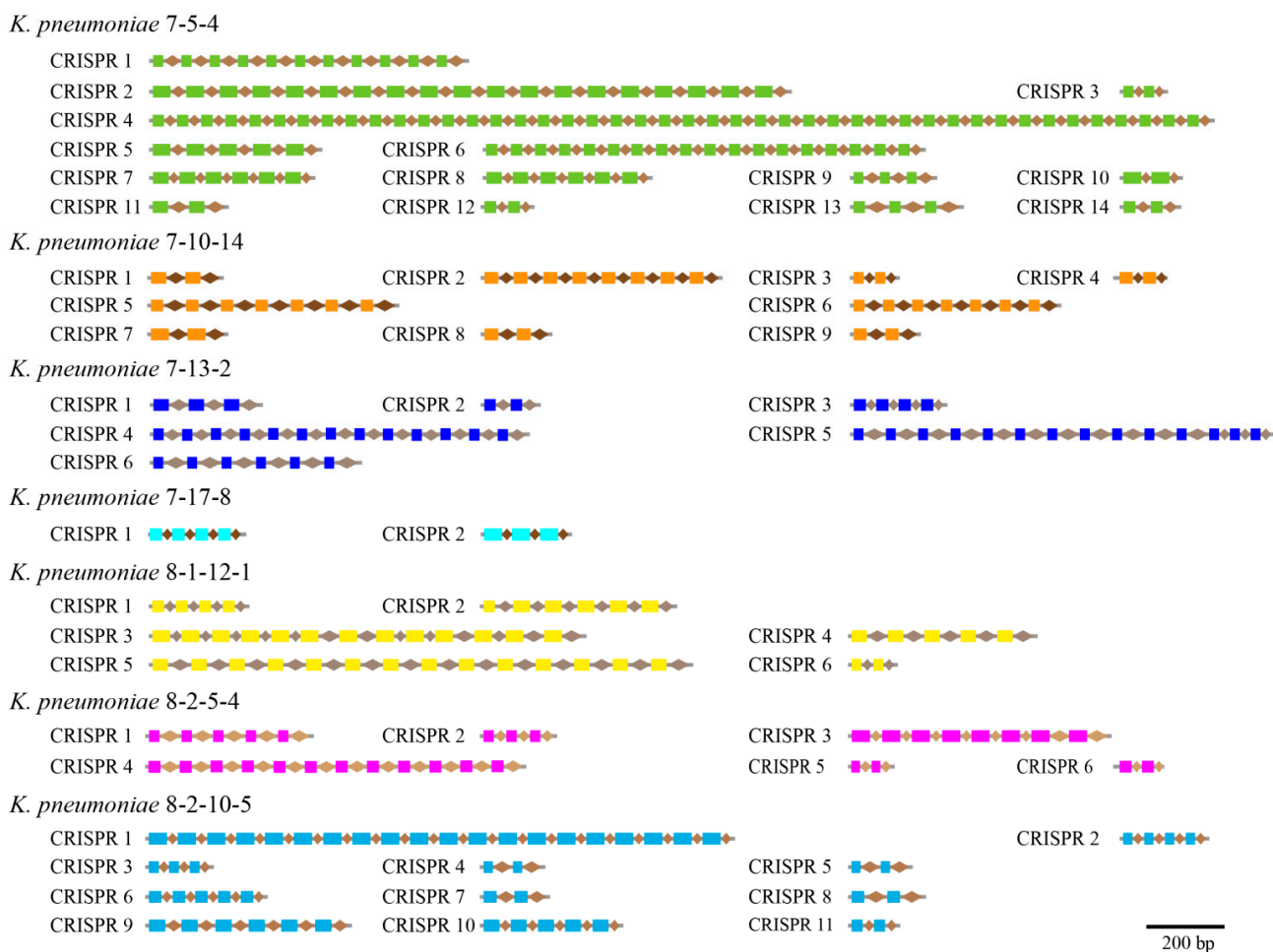


Figure 6. Structural features of the CRISPR repeats identified in the *K. pneumoniae* genomes. The repeat sequences were shown by the rectangle in different colors, and the spacer regions were represented by rhombuses in different colors.

The other virulence-related genes involved in the bacterial persistence in the host were also identified in the seven *K. pneumoniae* genomes. For example, the *fimH* gene encoding a fimbrial protein was found in the *K. pneumoniae* 7-5-4, 7-17-8, 8-1-12-1, 8-2-5-4, and 8-2-10-5 genomes, which can bind to highly mannoseylated UPIa to ensure stable adhesion of bacteria to tissues in the host [43].

Table 2. The putative virulence-related genes identified in the *K. pneumoniae* genomes.

Virulence-Related Gene	<i>K. pneumoniae</i> Genome	Reference
<i>ecpABCDEF</i>	7-5-4, 7-10-14, 7-13-2, 7-17-8, 8-1-12-1, 8-2-5-4, 8-2-10-5	[44]
<i>entABCDEFGS</i>	7-5-4, 7-10-14, 7-13-2, 7-17-8, 8-1-12-1, 8-2-5-4, 8-2-10-5	[45]
<i>fepABCDFG</i>	7-5-4, 7-10-14, 7-13-2, 7-17-8, 8-1-12-1, 8-2-5-4, 8-2-10-5	[46]
<i>fes</i>	7-5-4, 7-10-14, 7-13-2, 7-17-8, 8-1-12-1, 8-2-5-4, 8-2-10-5	[46]
<i>gnd</i>	7-5-4, 7-10-14, 7-13-2, 7-17-8, 8-1-12-1, 8-2-5-4, 8-2-10-5	[47]
<i>kdsA</i>	7-5-4, 7-10-14, 7-13-2, 7-17-8, 8-1-12-1, 8-2-5-4, 8-2-10-5	[48]
<i>rcsAB</i>	7-5-4, 7-10-14, 7-13-2, 7-17-8, 8-1-12-1, 8-2-5-4, 8-2-10-5	[45]
<i>tuf</i>	7-5-4, 7-10-14, 7-13-2, 7-17-8, 8-1-12-1, 8-2-5-4, 8-2-10-5	[49]
<i>wza</i>	7-5-4, 7-10-14, 7-13-2, 7-17-8, 8-1-12-1, 8-2-5-4, 8-2-10-5	[50]

Table 2. Cont.

Virulence-Related Gene	<i>K. pneumoniae</i> Genome	Reference
<i>galU</i>	7-10-14, 7-13-2, 7-17-8, 8-1-12-1, 8-2-5-4, 8-2-10-5	[51]
<i>hcp</i>	7-5-4, 7-10-14, 7-13-2, 7-17-8, 8-1-12-1, 8-2-5-4	[52]
<i>impBCGHJKL</i>	7-5-4, 7-10-14, 7-13-2, 7-17-8, 8-1-12-1, 8-2-5-4	[52,53]
<i>vasDG</i>	7-5-4, 7-10-14, 7-13-2, 7-17-8, 8-1-12-1, 8-2-5-4	[53]
<i>yhjH</i>	7-5-4, 7-10-14, 7-13-2, 7-17-8, 8-1-12-1, 8-2-5-4, 8-2-10-5	[54]
<i>fimABCDEFGI</i>	7-5-4, 7-13-2, 7-17-8, 8-1-12-1, 8-2-5-4, 8-2-10-5	[55]
<i>fimH</i>	7-5-4, 7-17-8, 8-1-12-1, 8-2-5-4, 8-2-10-5	[43]
<i>manBC</i>	7-5-4, 7-10-14, 7-17-8, 8-1-12-1, 8-2-5-4	[56]
<i>vgrG</i>	7-5-4, 7-10-14, 7-13-2, 8-1-12-1, 8-2-5-4	[57]
<i>iroE</i>	7-13-2, 7-17-8, 8-2-5-4, 8-2-10-5	[46]
<i>glf</i>	7-10-14, 7-13-2, 8-2-5-4	[58]
<i>vasJ</i>	7-10-14, 8-2-5-4	[59]
<i>fyuA</i>	7-17-8, 8-1-12-1	[60]
<i>irp12345</i>	7-17-8, 8-1-12-1	[55,61]
<i>mbtI</i>	7-17-8, 8-1-12-1	[62]
<i>ybtAX</i>	7-17-8, 8-1-12-1	[63,64]
<i>allABCDS</i>	8-2-10-5	[65]
<i>iucABCD</i>	8-2-5-4	[45]

3.7. Antibiotic and Heavy Metal Resistance-Associated Genes in the *K. pneumoniae* Genomes

Antimicrobial resistance-related genes ($n = 20–35$) were also identified in the 7 *K. pneumoniae* genomes (Table 3). *K. pneumoniae* 7-5-4 from *M. anguillicaudatus* contained the maximum number of such genes ($n = 35$), whereas *K. pneumoniae* 7-13-2, 7-17-8, and 8-1-12-1 isolates had the least ($n = 20$).

All the *K. pneumoniae* genomes contained the genes for MDR, e.g., a multidrug efflux SMR transporter subunit (*KpnE*), a spermidine export protein *mdtJ* (*KpnF*), a multidrug efflux MFS transporter periplasmic adaptor subunit *emrA* (*KpnG*), a multidrug resistance protein (*KpnH*), a multidrug efflux MFS transporter (*mdtG*), a multidrug efflux RND transporter permease subunit (*acrB*), a multidrug efflux RND transporter periplasmic adaptor subunit (*oqxA*), a multidrug efflux RND transporter permease subunit (*oqxB*), and a multidrug ABC transporter permease/ATP-binding protein (*yojI*).

The *qnrs1* gene, encoding a quinolone resistance pentapeptide repeat protein, was present in the *K. pneumoniae* 7-5-4 and 8-2-10-5 genomes, while the *floR*, *mphA*, and *sul1* genes were found in the *K. pneumoniae* 7-5-4, 7-10-14, and 8-2-10-5 genomes, which encoded a chloramphenicol/florfenicol efflux MFS transporter (*floR*), a *mphA* family macrolide 2-phosphotransferase (*mphA*), and a sulfonamide-resistant dihydropteroate synthase (*sul1*), respectively. Additionally, the genes involved in the resistance to β -lactam antibiotics (penicillins, cephalosporins, carbapenems, and monobactams) and aminoglycosides were also found in some of the *K. pneumoniae* genomes (Table 3). These results provided genome-wide evidence for antibiotic resistance phenotypes of the seven *K. pneumoniae* isolates.

Several genes involved in heavy metal tolerance were identified in the *K. pneumoniae* genomes as well (Table 3). For example, the *copA* gene, which plays a key role in the export of excess copper [66], was present in the seven *K. pneumoniae* genomes. Moreover, the *cusARS* genes, which are involved in the heavy metal efflux RND transporter [66,67], were also found in the seven *K. pneumoniae* genomes. Additionally, the *K. pneumoniae* 7-10-14 genome carried the *zntA* gene as well, which encodes a Zn/Cd/Hg/Pb-transporting ATPase, while *K. pneumoniae* 7-13-2 had the *arsABCR* genes, which are essential for heavy metal As resistance [68].

Table 3. The antibiotic and heavy metal resistance-related genes identified in the *K. pneumoniae* genomes.

Antibiotic/Heavy Metal	Gene	<i>K. pneumoniae</i> Genome	Reference
Cephalosporin	<i>acrB</i>	7-5-4, 7-10-14, 7-13-2, 7-17-8, 8-1-12-1, 8-2-5-4, 8-2-10-5	[69]
	Fluoroquinolone	<i>hns</i>	7-5-4, 7-10-14, 7-13-2, 7-17-8, 8-1-12-1, 8-2-5-4, 8-2-10-5
	<i>emrR</i>	7-5-4, 7-10-14, 7-13-2, 7-17-8, 8-1-12-1, 8-2-5-4, 8-2-10-5	[71]
	<i>marA</i>	7-5-4, 7-10-14, 7-13-2, 7-17-8, 8-1-12-1, 8-2-5-4, 8-2-10-5	[72]
	<i>ramA</i>	7-5-4, 7-10-14, 7-13-2, 7-17-8, 8-1-12-1, 8-2-5-4, 8-2-10-5	[72]
	<i>crp</i>	7-5-4, 7-10-14, 7-13-2, 7-17-8, 8-1-12-1, 8-2-5-4, 8-2-10-5	[73]
	<i>qnrS1</i>	7-5-4, 8-2-10-5	[74]
	<i>qnrB2</i>	7-10-14, 8-2-10-5	[75]
Tetracycline	<i>oqxAB</i>	7-5-4, 7-10-14, 7-13-2, 7-17-8, 8-1-12-1, 8-2-5-4, 8-2-10-5	[44]
	<i>tet(A)</i>	7-5-4, 7-10-14, 8-2-10-5, 8-2-5-4	[44]
Aminoglycoside	<i>KpnEFGH</i>	7-5-4, 7-10-14, 7-13-2, 7-17-8, 8-1-12-1, 8-2-5-4, 8-2-10-5	[76,77]
	<i>ompK37</i>	7-5-4, 7-10-14, 7-13-2, 7-17-8, 8-1-12-1, 8-2-5-4, 8-2-10-5	[78]
	<i>aph(3')-Ia</i>	7-5-4, 7-10-14, 8-2-10-5	[79]
	<i>aph(3'')-Ib</i>	7-5-4, 7-10-14, 8-2-10-5	[79]
	<i>aph(6)-Id</i>	7-5-4, 7-10-14, 8-2-10-5	[79]
	<i>aac(3)-IId</i>	7-10-14, 8-2-10-5	[79]
	<i>aac(6')-Ib-cr</i>	7-10-14, 8-2-10-5	[80]
	<i>aadA16</i>	7-10-14, 8-2-10-5	[79]
	<i>aadA8</i>	7-5-4	[81]
	<i>dfrA27</i>	7-10-14, 8-2-10-5	[82]
Diaminopyrimidine	<i>SHV-11</i>	7-5-4, 7-17-8	[83]
	<i>SHV-1</i>	7-10-14, 7-13-2	[84]
	<i>SHV-38</i>	8-1-12-1, 8-2-5-4	[85]
	<i>TEM-1</i>	7-5-4	[85]
	<i>OKP-B-7</i>	8-2-10-5	[86]
	<i>TEM-116</i>	8-2-5-4	[85]
Macrolide	<i>mphA</i>	7-5-4, 7-10-14, 8-2-10-5	[44]
	<i>ermB</i>	7-5-4	[44]
	<i>mphE</i>	7-5-4	[87]
	<i>msrE</i>	7-5-4	[87]
Nitroimidazole	<i>msbA</i>	7-5-4, 7-10-14, 7-13-2, 7-17-8, 8-1-12-1, 8-2-5-4, 8-2-10-5	[88]
	<i>floR</i>	7-5-4, 7-10-14, 8-2-10-5	[89]
Phenicol	<i>pmrF</i>	7-5-4, 7-10-14, 7-13-2, 7-17-8, 8-1-12-1, 8-2-5-4, 8-2-10-5	[90]
	<i>ugd</i>	7-5-4, 7-10-14, 7-13-2, 7-17-8, 8-1-12-1, 8-2-5-4, 8-2-10-5	[91]
	<i>yojI</i>	7-5-4, 7-10-14, 7-13-2, 7-17-8, 8-1-12-1, 8-2-5-4, 8-2-10-5	[92]
Peptide	<i>sul1</i>	7-5-4, 7-10-14, 8-2-10-5	[44]
	<i>sul2</i>	7-5-4, 8-2-10-5	[44]
Sulfonamide	<i>arr-2</i>	7-5-4	[80]
	<i>arr-3</i>	7-10-14	[46]
Rifamycin	<i>FosA5</i>	7-5-4, 7-10-14	[80]
	<i>FosA6</i>	7-13-2, 7-17-8, 8-1-12-1, 8-2-5-4, 8-2-10-5	[80]
	<i>mdtG</i>	7-5-4, 7-10-14, 7-13-2, 7-17-8, 8-1-12-1, 8-2-5-4, 8-2-10-5	[93]
Fosfomycin	<i>cusARS</i>	7-5-4, 7-10-14, 7-13-2, 7-17-8, 8-1-12-1, 8-2-5-4, 8-2-10-5	[66,67]
Heavy metal	<i>copA</i>	7-5-4, 7-10-14, 7-13-2, 7-17-8, 8-1-12-1, 8-2-5-4, 8-2-10-5	[66]
Heavy metal	<i>zntA</i>	7-10-14	[94]
Heavy metal	<i>arsABCR</i>	7-13-2	[68]

3.8. Strain-Specific Genes of the *K. pneumoniae* Isolates of Aquatic Animal Origins

Comparative genomic analyses revealed approximately 4111 core genes shared by the *K. pneumoniae* genomes, which accounted for 65.7% of pan genes ($n = 6255$). Meanwhile, many strain-specific genes ($n = 199–605$) were found in the *K. pneumoniae* isolates (Figure 7). Interestingly, *K. pneumoniae* 7-5-4 from *M. anguillicaudatus* contained the highest number of strain-specific genes ($n = 605$), whereas *K. pneumoniae* 7-10-14 from *T. veneriformis* had the fewest ($n = 199$). Remarkably, higher percentages of the strain-specific genes (30.2–54.4%) encoded unknown proteins. These results also provided the evidence of the considerable genome variation in the *K. pneumoniae* isolates of aquatic animal origins.

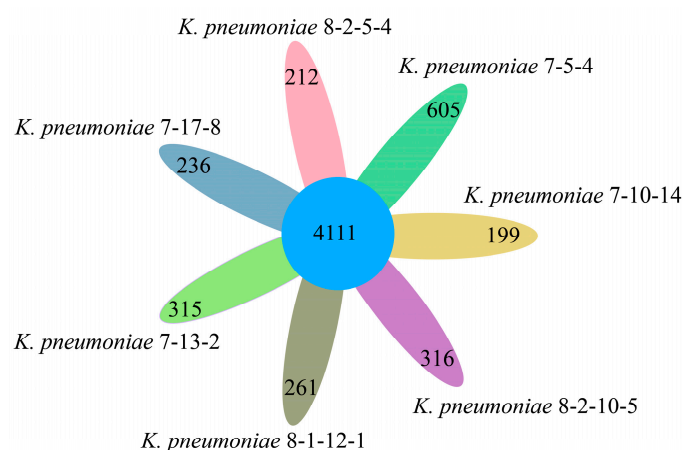


Figure 7. The Venn diagram showing the number of core genes and strain-specific genes in the seven *K. pneumoniae* genomes.

3.9. Phylogenetic Relatedness of the *K. pneumoniae* Isolates of Aquatic Animal Origins

To address phylogenetic relatedness of the *K. pneumoniae* isolates of aquatic animal origins, we constructed a phylogenetic tree on the basis of 72 *K. pneumoniae* genomes. Of these, complete genomes of 65 *K. pneumoniae* strains were derived from the GenBank database, the majority of which ($n = 57$) were isolated from human samples, followed by animals ($n = 5$, bovine, cat, chicken, dog, pig, and rabbit), and water environment ($n = 3$) in 1999–2021. The 7 *K. pneumoniae* isolates of aquatic animal origins tested negative for the toxic K1, K2, K5, K20, K54, and K57 serotypes, except *K. pneumoniae* 8-2-5-4 of serotype K2 [15]. The phylogenetic tree analysis revealed seven distinct clusters, designated as Clusters A–F (Figure 8).

K. pneumoniae 8-1-12-1 from *P. clarkii* fell into Cluster B, together with *K. pneumoniae* JX-CR-hvKP (GenBank accession no. NZ_CP064208), which was isolated from human blood in 2019 in China.

Both *K. pneumoniae* 7-10-14 from *M. Veneriformis* and *K. pneumoniae* 7-17-8 from *C. cahayensis* were classified into Cluster F, together with *K. pneumoniae* 49,210 (GenBank accession no. NZ_CP089024) isolated from humans in 2016 in China.

Both *K. pneumoniae* 7-5-4 from *M. anguillicaudatus* and *K. pneumoniae* 8-2-10-5 from *E. fuscoguttatus* were grouped into Cluster E, together with *K. pneumoniae* SWHE3 (GenBank accession no. NZ_CP055061) isolated from humans in 2018 in China, and *K. pneumoniae* SB617 (GenBank accession no. NZ_CP084825), which was isolated from water in 2000 in the Netherlands.

K. pneumoniae 7-13-2 from *E. sinensis* was classified into a single Cluster A, phylogenetically distant from all the other genomes tested, suggesting its unique genome trait.

K. pneumoniae 8-2-5-4 of serotype K2 from *T. granosa* was classified into Cluster D, showing the closest phylogenetic distance with *K. pneumoniae* BcKp067 (GenBank accession no. NZ_CP084829), which was isolated from the water environment in 1999 in the Netherlands.

In addition, 8 *K. pneumoniae* isolates belonging to the capsule serotypes K1, K2, K5, K54 and K57 were classified into Clusters D–F.

Taken together, these results demonstrated the genome diversity of the *K. pneumoniae* isolates of the clinical and environmental origins.

3.10. Sequence Types (ST) of the *K. pneumoniae* Isolates of Aquatic Animal Origins

Based on the 7 conserved core genes (*gapA*, *infB*, *mdh*, *pgi*, *phoE*, *rpoB*, and *tonB*) in *K. pneumoniae* [15], the multilocus sequence typing (MLST) analysis against the MLST database (<https://cge.food.dtu.dk/services/MLST/> (accessed on 23 November 2022)) revealed that *K. pneumoniae* 7-5-4, 7-10-14, 7-13-2, 7-17-8, 8-1-12-1, and 8-2-5-4 isolates belonged to the ST-273, ST-1310, ST-101, ST-353, ST-6289, and ST-2026, respectively, whereas the *K. pneumoniae* 8-2-10-5 isolate was not classified into any known STs.

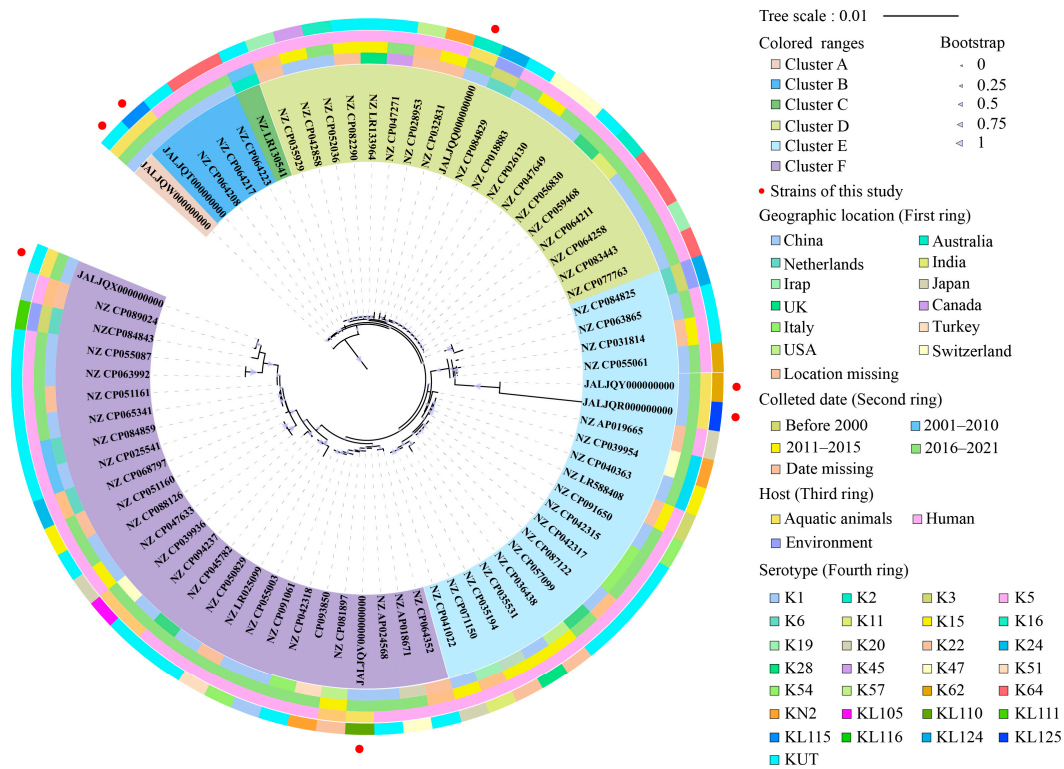


Figure 8. The phylogenetic tree showing the relationship of the 72 *K. pneumoniae* genomes. Complete genome sequences of the 65 *K. pneumoniae* isolates were retrieved from the GenBank database with accession numbers shown in the tree. The seven *K. pneumoniae* genomes determined in this study were marked with red dots. The maximum likelihood method was used to build a tree, with 1000 bootstrap replications and a cut-off threshold of $\geq 50\%$ bootstrap values.

4. Discussion

The inappropriate use of antibiotics may result in increasing levels of bacterial resistance [8,95]. For example, Fatima et al. [96] examined the resistance of *K. pneumoniae* isolates from urine ($n = 72$) and sputum ($n = 35$) isolated in Balochistan to 17 antimicrobial agents. They found that the majority of the *K. pneumoniae* isolates were resistant to GEN (76.2%), followed by SXT (66.7%), and NOR (42.9%) [96]. Marques et al. [97] determined the resistance of *K. pneumoniae* isolates from companion animals ($n = 27$) and humans ($n = 77$), isolated in Lisbon during 2002 to 2015, to 29 antimicrobial agents. Their results showed that most *K. pneumoniae* isolates were resistant to AMP (95.2%), followed by CHL (31.7%), KAN (27.9%), TET (28.8%), and CIP (25%) [97]. In this study, the *K. pneumoniae* isolates had different antibiotic resistance profiles. For example, *K. pneumoniae* 7-5-4 from *M. anguillicaudatus* and *K. pneumoniae* 7-10-14 from *M. veneriformis* displayed resistance to CHL/CIP/KAN/NOR/SXT/TET and AMP/CHL/GEN/KAN/SXT/TET, respectively. *K. pneumoniae* 8-2-10-5 from *E. fuscoguttatus* was resistant to CHL/CIP/KAN/SXT/TET, while *K. pneumoniae* 8-2-5-4 from *T. granosa* was resistant to AMP/CHL/TET, suggesting different antibiotic exposure levels or pollution sources of aquaculture environments.

Previous studies have reported heavy metal residues in various aquatic environments and aquatic products sampled around the world, especially in developing countries [98,99]. For example, Varol and Sunbul et al. [98] examined the residues of five heavy metals in biota samples, including one species of mussel, crayfish, and farmed fish, respectively, and six species of wild fish, collected from the Euphrates River in Turkey. The highest concentrations of As, Cd, and Pb were detected in mussels, while the highest concentrations of Cu and Zn were detected in crayfish [98]. Recently, Ni et al. [99] reported Cu, Hg, Pb, and Cd residues in 41 species of aquatic animals, sampled in Shanghai, China in July–September of 2018–2019, with positive sample rates of 100%, 100%, 77.4%, and 34.0%, respectively, but

none of which exceeded their maximum residue limits [99]. In this study, the *K. pneumoniae* isolates had different heavy metal tolerance patterns. For example, *K. pneumoniae* 8-1-12-1 from *P. clarkii* was tolerant to $\text{Cu}^{2+}/\text{Cd}^{2+}/\text{Cr}^{3+}/\text{Hg}^{2+}/\text{Mn}^{2+}/\text{Pb}^{2+}/\text{Zn}^{2+}$, while *K. pneumoniae* 8-2-10-5 from *E. fuscoguttatus* was tolerant to $\text{Zn}^{2+}/\text{Pb}^{2+}/\text{Hg}^{2+}/\text{Cu}^{2+}/\text{Cr}^{3+}/\text{Cd}^{2+}$. These results suggested a potential risk of consuming these aquatic animals.

The human acidic stomach environment challenges survival and infection of *K. pneumoniae*. Therefore, we examined survival of the *K. pneumoniae* isolates at pH 3.5–7.5 when incubated in the TSB (0.5% NaCl) at 37 °C. Unexpectedly, all the isolates were capable of growing vigorously at pH 4.5–7.5, although the highest biomass was observed at pH 7.5. These results provided evidence of the acidic tolerance of the *K. pneumoniae* isolates of animal origins, which may have been attributed to the bacterial survival across the acidic stomach boundary in the host.

The *K. pneumoniae* isolates were recovered from different aquatic animals in water environments. *M. anguillicaudatus*, *E. sinensis*, *C. cahayensis*, and *P. clarkii* were derived from freshwater, while *M. Veneriformis*, *T. granosa*, and *E. fuscoguttatus* from seawater. Therefore, we determined growth curves of the *K. pneumoniae* isolates at different salinity concentrations (0.5–4% NaCl) when incubated in the TSB (pH 7.5) at 37 °C. Our results indicated that all the *K. pneumoniae* isolates were able to grow vigorously at 0.5–1.0% NaCl in the TSB (pH 7.5) at 37 °C. Of these, *K. pneumoniae* 7-5-4 from *M. anguillicaudatus* was the most susceptible to higher salinity concentrations (4–3% NaCl), consistent with its freshwater culture environment.

Draft genomes of the seven *K. pneumoniae* isolates were determined using the Illumina HiSeq × Ten sequencing platform. The typical Poisson distribution, with a clear single peak at the only 17-mers frequency, was observed in the sequencing data, indicating less repetitive DNA in the *K. pneumoniae* genomes (Figure S1, Table S9). The assembled genomes were 5,256,522–5,857,823 bp with GC contents of 56.35–57.81%, similar to the other *K. pneumoniae* genomes [42,100]. For example, Yu et al. [100] used MiSeq short-read sequencing and Oxford nanopore long-read sequencing to determine whole genomes of 7 CRKP strains, and obtained genome sizes ranging from 5.4 to 5.8 Mb with an average GC content of 57.2% [100]. Du et al. [42] sequenced and de novo assembled the genomes of 6 hvKP strains, which ranged 5.34–5.58 Mb and GC percentages ranging from 57.22 to 57.46% [42]. The genome sizes of 1757 *K. pneumoniae* strains, which were available in the GenBank database (accessed on 14 March, 2023), ranged from 4.76 Mb to 6.37 Mb, most of which contained 3107 to 5973 predicted genes. In this study, interestingly, a total of 4885–5558 protein-coding genes were predicted, of which 1188–1363 protein-coding genes encoded unknown proteins. Moreover, about 7.1–41.0% of the strain-specific ($n = 199$ –605) genes encoded unknown proteins as well. These results highlighted specific genome traits of the *K. pneumoniae* isolates of aquatic animal origins, which may result from the high numbers of identified MGEs.

Remarkably, the *K. pneumoniae* genomes carried many MGEs, including GIs ($n = 87$), prophages ($n = 14$), INs ($n = 4$), and ISs ($n = 22$). The identified MGEs carrying a large number of genes may constitute an important driving force in *K. pneumoniae* genome evolution and speciation. For instance, the identified 87 GIs endowed the bacterium with a variety of biological functions for fitness into niches, such as virulence, resistance, substrate hydrolysis, transporting and utilization, and restriction and modification, as well as phage and stress regulation.

There are approximately 10^{31} bacteriophages on earth, which play a critical role in virulence and evolution of bacterial genomes [101]. Bleriot et al. [102] reported 40 prophages (11.454–84.199 kb) in 16 clinical CRKP strains, 27 of which belonged to the family *Myoviridae*, 10 to *Siphoviridae*, and 3 to *Podoviridae* [102]. In this study, we found 14 prophages (12,633–109,928 bp) in the 7 *K. pneumoniae* genomes, which were derived from different genera, including *Enterobacteria*, *Klebsiella*, *Pseudomonas*, and *Ralstonia*. The results in this study, coupled with previous report [102], indicated extensive phage transmission between *Klebsiella* and the other bacterial genera. In this study, the identified prophage homologues,

e.g., *Enterobacteria_phage_186*, *Klebsiella_phage_phiKO2*, and *Pseudomonas_phage_D3*, were present in different *K. pneumoniae* genomes, but in different lengths encoding different numbers of genes, which provided evidence of extensive genome rearrangement during the *K. pneumoniae* evolution.

It has been reported that the Type 1 IN is the most prevalent and common in clinical bacteria [103]. For example, Firoozeh et al. [104] isolated *K. pneumoniae* strains ($n = 181$) from clinical specimens and found 82.9% ($n = 150$) of the isolates with MDR phenotypes. Of the MDR isolates, 100% ($n = 150$) and 36.7% ($n = 55$) carried *intI1* and *intI2* genes, respectively, but none had the *intI3* gene by PCR amplification [104]. In this study, 4 INs (1229–4332 bp) were identified in the *K. pneumoniae* 7-5-4, 7-10-14, and 8-2-10-5 genomes. Of these, *K. pneumoniae* 7-5-4 carried the Type 1 IN. Moreover, this IN contained ARGs, encoding a NAD(+)-rifampin ADP-ribosyltransferase *arr-2* (*Kp_7_5_4_5567*) and an ANT(3'')-Ia family aminoglycoside nucleotidyltransferase *aadA3* (*Kp_7_5_4_5566*), suggesting possible transmission of ARGs mediated by the IN.

ISs consist of two inverted repeat sequences and one or two genes encoding transposases [105]. In this study, all the 7 *K. pneumoniae* genomes contained ISs ($n = 2$ to 6), ranging from 741 to 1588 bp. They belonged to the IS3 family, IS5 family, IS6 family, IS91 family, and IS110 family.

The CRISPR-Cas systems defend the prokaryotes from invasion by MGEs [106]. In this study, 54 CRISPR-Cas gene clusters (75–2649 bp) were identified in the 7 *K. pneumoniae* genomes. However, all the predicted clusters lacked the Cas protein, which plays an essential role in the function of the CRISPR-Cas systems [107]. These results provided indirect evidence for inactive CRISPR-Cas repeats and possible active HGT in the 7 *K. pneumoniae* isolates.

Many virulence-related genes have been identified in *K. pneumoniae* isolates [108,109]. For example, Remya et al. [108] detected 9 virulence genes in *K. pneumoniae* isolates ($n = 370$) by PCR amplification, including the *magA*, *allS*, *kfu*, *K2A*, *rmpA*, *entB*, *ybtS*, *fimH*, and *uge* genes. They found that 93.2% (345/370) of the isolates carried multiple virulence genes, 4.0% (15/370) carried 1, and 2.7% (10/370) had none [108]. Kuş et al. [109] detected 16 virulence genes in *K. pneumoniae* strains ($n = 53$) isolated from nosocomial infections in Turkey by PCR amplification, including the *fimH-1*, *mrkD*, *kpn*, *iutA*, *ycfM*, *entB*, *irp-1*, *irp-2*, *ybtS*, *fyuA*, *iroN*, *rmpA*, *magA*, *traT*, *hlyA*, and *cnf-1* genes. Their results showed that the *entB* gene was the most predominant (96.2%), followed by the *ycfM* (86.8%), *mrkD* (83.0%), *fimH-1* (64.2%), *fyuA* (54.7%), and *kpn* (49.1%). The detection rates of the *ybtS*, *irp-1*, *irp-2*, *traT*, and *iutA* genes ranged from 41.5 to 5.7%, whereas the other genes (*iroN*, *rmpA*, *magA*, *hlyA*, and *cnf-1*) tested negative in the isolates [109]. In this study, based on the obtained genome sequences, we also identified many virulence-related genes ($n = 43$ –59) in the 7 *K. pneumoniae* isolates of aquatic animal origins, e.g., *ecpABCDE*, *entABCDEFG*, *fimABCDEFGH*, *iucABCD*, *fepABCDG*, *fyuA*, *vgrG*, *galU*, *gnd*, *vgrG*, *fimH*, *entB*, *mrkD*, *ybtA*, and T6SS-associated genes, which were involved in adhesion, antiphagocytosis, secretion system, and gene regulation of *K. pneumoniae*. Of note, *K. pneumoniae* 8-1-12-1 from *P. clarkii* contained the maximum number of the virulence-associated genes ($n = 59$), whereas *K. pneumoniae* 7-10-14 from *M. veneriformis* had relatively fewer ($n = 43$). These virulence-related genes may be candidate targets for the development of new diagnostics, vaccines, and treatments to control *K. pneumoniae* infection.

The emergence and spread of MDR pathogens poses a serious threat to public safety [110]. For example, Marques et al. [97] reported 15 antibiotic resistance-related genes in *K. pneumoniae* isolates, causing UTIs from companion animals ($n = 27$) and humans ($n = 77$), e.g., *qnrB*, *qnrS*, *sul1*, *sul2*, *sul3*, *dfrA12*, *dfrIa*, *tet(A)*, *tet(B)*, and *floR* [97]. In this study, many antibiotic resistance-related genes ($n = 20$ –35) were identified in the 7 *K. pneumoniae* genomes, e.g., *tetA*, *acrB*, *hns*, *oqxA*, *aac (6')-Ib-cr*, *ermB*, *msbA*, *floR*, *pmrF*, *sul1*, *arr-2*, and *fosA5*, which are involved in the resistance to cephalosporin, fluoroquinolone, tetracycline, aminoglycoside, macrolide, phenicol, sulfonamide, rifamycin, and fosfomycin. Moreover, several genes in heavy metal tolerance were also identified in the seven *K. pneumoniae* genomes, such as

the *cusASR*, *copA*, *zntA*, and *arsABCR* genes. These results provided genome-wide evidence for the resistance phenotypes of the *K. pneumoniae* isolates of aquatic animal origins.

5. Conclusions

The *K. pneumoniae* 7-10-14, 7-17-8, 8-2-5-4, 7-13-2, 8-1-12-1, 8-2-10-5, and 7-5-4 strains of aquatic animal origins had multiple antibiotic resistance and heavy metal tolerance profiles, and were capable of growing vigorously at pH 4.5–7.5 and 0.5–1.0% NaCl in the TSB medium at 37 °C.

Remarkably, the *K. pneumoniae* genomes carried many MGEs, including GIs ($n = 87$), prophages ($n = 14$), INs ($n = 4$), and ISs ($n = 22$), as well as partial or inactive CRISPR-Cas systems ($n = 54$), indicating possible active HGT during the *K. pneumoniae* genome evolution. Many antibiotic resistance ($n = 20–35$) and virulence ($n = 43–59$)-related genes were found in the *K. pneumoniae* genomes. *K. pneumoniae* 7-5-4 from *M. anguillicaudatus* contained the maximum number of ARGs ($n = 35$), while *K. pneumoniae* 8-1-12-1 from *P. clarkii* carried the most virulence-related genes ($n = 59$). Additionally, numerous strain-specific ($n = 199–605$) genes were present in the *K. pneumoniae* isolates, approximately 30.2–54.4% of which encoded unknown proteins. These results, coupled with the phylogenetic tree analysis, demonstrated considerable genome variation and high genome plasticity of the *K. pneumoniae* isolates.

Overall, the results of this study enrich genome data and fill prior gaps in understanding the *K. pneumoniae* genomes derived from aquatic animals.

Supplementary Materials: The following supporting information can be downloaded at: <https://www.mdpi.com/article/10.3390/d15040527/s1>, Table S1: The genotypes and phenotypes of the *K. pneumoniae* isolates used in this study; Table S2: The oligonucleotide primers used in this study; Table S3: The sixty-five *K. pneumoniae* strains with complete genomes used in the phylogenetic tree; Table S4: The identified GIs in the *K. pneumoniae* genomes; Table S5: Various functions of the identified GIs in the *K. pneumoniae* genomes; Table S6: The identified prophages in the *K. pneumoniae* genomes; Table S7: The identified INs in the *K. pneumoniae* genomes; Table S8: The identified ISs in the *K. pneumoniae* genomes; Table S9: The identified repeats at the end of scaffolds of the *K. pneumoniae* genomes; Figure S1: The k-mer analysis for *K. pneumoniae* subread data based on the number of unique 17-mers; (A–G): *K. pneumoniae* 7-5-4, 7-10-14, 7-13-2, 7-17-8, 8-1-12-1, 8-2-5-4, and 8-2-10-5 genomes, respectively; Figure S2: Genome circle maps of the seven *K. pneumoniae* isolates. Circles from the inwards to outside represented GC content (outward parts mean higher than average, while inward parts mean lower than average); GC-skew (purple values are higher than zero, while green values are lower than zero); the reference genome of *K. pneumoniae* ATCC43816 (GenBank accession no. NZ_CP064352); *K. pneumoniae* 8-2-5-4, 8-2-10-5, 8-1-12-1, 7-17-8, 7-13-2, 7-10-14, and 7-5-4 genomes, respectively; and CDSs on the negative and positive chains (inward and outward parts), respectively. References [111–113] are cited in the supplementary materials.

Author Contributions: H.G.: investigation, data curation, and writing—original draft preparation; L.X.: supervision and discussion; L.C.: funding acquisition, conceptualization, and writing—review and editing. All authors have read and agreed to the published version of the manuscript.

Funding: This study was supported by the Shanghai Municipal Science and Technology Commission, grant number 17050502200, and the National Natural Science Foundation of China, grant number 31671946.

Institutional Review Board Statement: Not applicable.

Data Availability Statement: Draft genome sequences of the seven *K. pneumoniae* isolates have been deposited in GenBank database under the accession numbers: JALJQY000000000, JALJQX000000000, JALJQW000000000, JALJQV000000000, JALJQT000000000, JALJQQ000000000, and JALJQR000000000.

Acknowledgments: The authors are grateful to Dingxiang Xu at Shanghai Ocean University for help with the genome sequence analysis in this study.

Conflicts of Interest: The authors declare no conflict of interest.

References

1. Martin, R.M.; Bachman, M.A. Colonization, infection, and the accessory genome of *Klebsiella pneumoniae*. *Front. Cell Infect. Microbiol.* **2018**, *8*, 4. [[CrossRef](#)] [[PubMed](#)]
2. Girometti, N.; Lewis, R.E.; Giannella, M.; Ambretti, S.; Bartoletti, M.; Tedeschi, S.; Tumietto, F.; Cristini, F.; Trapani, F.; Gaibani, P.; et al. *Klebsiella pneumoniae* bloodstream infection: Epidemiology and impact of inappropriate empirical therapy. *Medicine* **2014**, *93*, 298–309. [[CrossRef](#)]
3. Paczosa, M.K.; Meccas, J. *Klebsiella pneumoniae*: Going on the offense with a strong defense. *Microbiol. Mol. Biol. Rev.* **2016**, *80*, 629–661. [[CrossRef](#)] [[PubMed](#)]
4. Arato, V.; Raso, M.M.; Gasperini, G.; Berlanda Scorza, F.; Micoli, F. Prophylaxis and treatment against *Klebsiella pneumoniae*: Current insights on this emerging anti-microbial resistant global threat. *Int. J. Mol. Sci.* **2021**, *22*, 4042. [[CrossRef](#)]
5. Turton, J.F.; Perry, C.; Elgohari, S.; Hampton, C.V. PCR characterization and typing of *Klebsiella pneumoniae* using capsular type-specific, variable number tandem repeat and virulence gene targets. *J. Med. Microbiol.* **2010**, *59*, 541–547. [[CrossRef](#)] [[PubMed](#)]
6. Li, B.; Zhao, Y.; Liu, C.; Chen, Z.; Zhou, D. Molecular pathogenesis of *Klebsiella pneumoniae*. *Future Microbiol.* **2014**, *9*, 1071–1081. [[CrossRef](#)]
7. Qin, X.; Wu, S.; Hao, M.; Zhu, J.; Ding, B.; Yang, Y. The colonization of carbapenem-resistant *Klebsiella pneumoniae*: Epidemiology, resistance mechanisms, and risk factors in patients admitted to intensive care units in China. *J. Infect. Dis.* **2020**, *221*, S206–S214. [[CrossRef](#)]
8. Liu, P.; Li, X.; Luo, M.; Xu, X.; Su, K.; Chen, S. Risk factors for carbapenem-resistant *Klebsiella pneumoniae* infection: A meta-analysis. *Microb. Drug Resist.* **2018**, *24*, 190–198. [[CrossRef](#)]
9. Galler, H.; Feierl, G.; Peternel, C.; Reinthaler, F.F.; Haas, D.; Grisold, A.J. KPC-2 and OXA-48 carbapenemase-harboring *Enterobacteriaceae* detected in an Austrian wastewater treatment plant. *Clin. Microbiol. Infect.* **2014**, *20*, O132–O134. [[CrossRef](#)]
10. Oliveira, S.; Moura, R.A.; Silva, K.C.; Pavez, M.; McCulloch, J.A.; Dropa, M. Isolation of KPC-2-producing *Klebsiella pneumoniae* strains belonging to the high-risk multiresistant clonal complex 11 (ST437 and ST340) in urban rivers. *J. Antimicrob. Chemother.* **2014**, *69*, 849–852. [[CrossRef](#)]
11. Jelić, M.; Hrenović, J.; Dekić, S.; Goić-Barišić, I.; Tambić Andrašević, A. First evidence of KPC-producing ST258 *Klebsiella pneumoniae* in river water. *J. Hosp. Infect.* **2019**, *103*, 147–150. [[CrossRef](#)] [[PubMed](#)]
12. Aguilar, S.; Rosado, D.; Moreno-Andrés, J.; Cartuche, L.; Cruz, D.; Acevedo-Merino, A. Inactivation of a wild isolated *Klebsiella pneumoniae* by photo-chemical processes: UV-C, UV-C/H₂O₂ and UV-C/H₂O₂/Fe³⁺. *Catal. Today.* **2018**, *313*, 94–99. [[CrossRef](#)]
13. Chen, J.; Sun, R.; Pan, C.; Sun, Y.; Mai, B.; Li, Q.X. Antibiotics and food safety in aquaculture. *J. Agric. Food Chem.* **2020**, *68*, 11908–11919. [[CrossRef](#)] [[PubMed](#)]
14. Luo, L.; Lu, S.; Huang, C.; Wang, F.; Ren, Y.; Cao, H. A survey of chloramphenicol residues in aquatic products of Shenzhen, South China. *Food Addit. Contam. Part A* **2021**, *38*, 914–921. [[CrossRef](#)] [[PubMed](#)]
15. Xu, Y.; Ni, L.; Guan, H.; Chen, D.; Qin, S.; Chen, L. First report of potentially pathogenic *Klebsiella pneumoniae* from serotype K2 in Mollusk *Tegillarca granosa* and genetic diversity of *Klebsiella pneumoniae* in 14 species of edible aquatic animals. *Foods* **2022**, *11*, 4058. [[CrossRef](#)]
16. Pal, A.; Bhattacharjee, S.; Saha, J.; Sarkar, M.; Mandal, P. Bacterial survival strategies and responses under heavy metal stress: A comprehensive overview. *Crit. Rev. Microbiol.* **2022**, *48*, 327–355. [[CrossRef](#)]
17. Jiang, H.; Yu, T.; Yang, Y.; Yu, S.; Wu, J.; Lin, R.; Li, Y.; Fang, J.; Zhu, C. Co-occurrence of antibiotic and heavy metal resistance and sequence type diversity of *Vibrio parahaemolyticus* isolated from *Penaeus vannamei* at freshwater farms, seawater farms, and markets in Zhejiang Province, China. *Front. Microbiol.* **2020**, *11*, 1294. [[CrossRef](#)]
18. Balali-Mood, M.; Naseri, K.; Tahergorabi, Z.; Khazdair, M.R.; Sadeghi, M. Toxic mechanisms of five heavy metals: Mercury, lead, chromium, cadmium, and arsenic. *Front. Pharmacol.* **2021**, *12*, 643972. [[CrossRef](#)]
19. Dickinson, A.W.; Power, A.; Hansen, M.G.; Brandt, K.K.; Piliposian, G.; Appleby, P. Heavy metal pollution and co-selection for antibiotic resistance: A microbial palaeontology approach. *Environ. Int.* **2019**, *132*, 105117. [[CrossRef](#)]
20. Kunhikannan, S.; Thomas, C.J.; Franks, A.E.; Mahadevaiah, S.; Kumar, S.; Petrovski, S. Environmental hotspots for antibiotic resistance genes. *Microbiologyopen* **2021**, *10*, e1197. [[CrossRef](#)]
21. Xu, D.; Peng, X.; Xie, L.; Chen, L. Survival and genome diversity of *Vibrio parahaemolyticus* isolated from edible aquatic animals. *Diversity* **2022**, *14*, 350. [[CrossRef](#)]
22. Chen, D.; Li, X.; Ni, L.; Xu, D.; Xu, Y.; Ding, Y.; Xie, L.; Chen, L. First experimental evidence for the presence of potentially toxic *Vibrio cholerae* in snails, and virulence, cross-resistance and genetic diversity of the bacterium in 36 species of aquatic food animals. *Antibiotics* **2021**, *10*, 412. [[CrossRef](#)] [[PubMed](#)]
23. Sun, X.; Liu, T.; Peng, X.; Chen, L. Insights into *Vibrio parahaemolyticus* CHN25 response to artificial gastric fluid stress by transcriptomic analysis. *Int. J. Mol. Sci.* **2014**, *15*, 22539–22562. [[CrossRef](#)] [[PubMed](#)]
24. Yang, L.; Wang, Y.; Yu, P.; Ren, S.; Zhu, Z.; Jin, Y.; Yan, J.; Peng, X.; Chen, L. Prophage-related gene VpaChn25_0724 contributes to cell membrane integrity and growth of *Vibrio parahaemolyticus* CHN25. *Front. Cell. Infect. Microbiol.* **2020**, *10*, 595709. [[CrossRef](#)]
25. Luo, R.; Liu, B.; Xie, Y.; Li, Z.; Huang, W.; Yuan, J.; He, G.; Chen, Y.; Pan, Q.; Liu, Y.; et al. SOAPdenovo2: An empirically improved memory-efficient short-read de novo assembler. *GigaScience* **2012**, *1*, 18. [[CrossRef](#)]

26. Delcher, A.L.; Bratke, K.A.; Powers, E.C.; Salzberg, S.L. Identifying bacterial genes and endosymbiont DNA with Glimmer. *Bioinformatics* **2007**, *23*, 673–679. [[CrossRef](#)]
27. Chan, P.P.; Lowe, T.M. tRNAscan-SE: Searching for tRNA genes in genomic sequences. *Methods Mol. Biol.* **2019**, *1962*, 1–14. [[CrossRef](#)]
28. Bertelli, C.; Laird, M.R.; Williams, K.P.; Lau, B.Y.; Hoad, G.; Winsor, G.L.; Brinkman, F.S.L. IslandViewer 4: Expanded prediction of genomic islands for larger-scale datasets. *Nucleic Acids Res.* **2017**, *45*, W30–W35. [[CrossRef](#)]
29. Fouts, D.E. Phage_Finder: Automated identification and classification of prophage regions in complete bacterial genome sequences. *Nucleic Acids Res.* **2006**, *34*, 5839–5851. [[CrossRef](#)]
30. Bland, C.; Ramsey, T.L.; Sabree, F.; Lowe, M.; Brown, K.; Kyrpides, N.C.; Hugenholtz, P. CRISPR recognition tool (CRT): A tool for automatic detection of clustered regularly interspaced palindromic repeats. *BMC Bioinform.* **2007**, *8*, 209. [[CrossRef](#)]
31. Cury, J.; Jové, T.; Touchon, M.; Néron, B.; Rocha, E.P. Identification and analysis of integrons and cassette arrays in bacterial genomes. *Nucleic Acids Res.* **2016**, *44*, 4539–4550. [[CrossRef](#)] [[PubMed](#)]
32. Siguier, P.; Gourbeyre, E.; Chandler, M. Bacterial insertion sequences: Their genomic impact and diversity. *FEMS Microbiol. Rev.* **2014**, *38*, 865–891. [[CrossRef](#)] [[PubMed](#)]
33. Stamatakis, A. RAxML version 8: A tool for phylogenetic analysis and post-analysis of large phylogenies. *Bioinformatics* **2014**, *30*, 1312–1313. [[CrossRef](#)] [[PubMed](#)]
34. Hu, Y.Y.; Liu, C.X.; Liu, P.; Wu, Z.Y.; Zhang, Y.D.; Xiong, X.S. Regulation of gene expression of hcp, a core gene of the type VI secretion system in *Acinetobacter baumannii* causing respiratory tract infection. *J. Med. Microbiol.* **2018**, *67*, 945–951. [[CrossRef](#)] [[PubMed](#)]
35. Chen, X.; Wei, Y.; Ji, X. Research progress of prophages. *Yi Chuan* **2021**, *43*, 240–248. [[CrossRef](#)]
36. Li, Y.; Yang, L.; Fu, J.; Yan, M.; Chen, D.; Zhang, L. Genotyping and high flux sequencing of the bacterial pathogenic elements-integrons. *Microb. Pathog.* **2018**, *116*, 22–25. [[CrossRef](#)]
37. Huyan, J.; Tian, Z.; Zhang, Y.; Zhang, H.; Shi, Y.; Gillings, M.R. Dynamics of class 1 integrons in aerobic biofilm reactors spiked with antibiotics. *Environ. Int.* **2020**, *140*, 105816. [[CrossRef](#)]
38. Partridge, S.R.; Kwong, S.M.; Firth, N.; Jensen, S.O. Mobile genetic elements associated with antimicrobial resistance. *Clin. Microbiol. Rev.* **2018**, *31*, e00088–17. [[CrossRef](#)]
39. Yu, Z.; Jiang, S.; Wang, Y.; Tian, X.; Zhao, P.; Xu, J. CRISPR-Cas adaptive immune systems in *Sulfolobales*: Genetic studies and molecular mechanisms. *Sci. China Life Sci.* **2021**, *64*, 678–696. [[CrossRef](#)]
40. Wang, G.; Song, G.; Xu, Y. Association of CRISPR/Cas system with the drug resistance in *Klebsiella pneumoniae*. *Infect. Drug Resist.* **2020**, *13*, 1929–1935. [[CrossRef](#)]
41. Kamruzzaman, M.; Iredell, J.R. CRISPR-Cas system in antibiotic resistance plasmids in *Klebsiella pneumoniae*. *Front. Microbiol.* **2020**, *10*, 2934. [[CrossRef](#)] [[PubMed](#)]
42. Du, L.; Zhang, J.; Liu, P.; Li, X.; Su, K.; Yuan, L. Genome sequencing and comparative genome analysis of 6 hypervirulent *Klebsiella pneumoniae* strains isolated in China. *Arch. Microbiol.* **2021**, *203*, 3125–3133. [[CrossRef](#)] [[PubMed](#)]
43. Sarshar, M.; Behzadi, P.; Ambrosi, C.; Zagaglia, C.; Palamara, A.T.; Scribano, D. FimH and anti-adhesive therapeutics: A disarming strategy against uropathogens. *Antibiotics* **2020**, *9*, 397. [[CrossRef](#)] [[PubMed](#)]
44. Shin, H.; Kim, Y.; Han, D.; Hur, H.G. Emergence of high level carbapenem and extensively drug resistant *Escherichia coli* ST746 producing NDM-5 in influent of wastewater treatment plant, seoul, South Korea. *Front. Microbiol.* **2021**, *12*, 645411. [[CrossRef](#)]
45. Yuan, L.; Li, X.; Du, L.; Su, K.; Zhang, J.; Liu, P. *RcsAB* and *fur* coregulate the iron-acquisition system via *entC* in *Klebsiella pneumoniae* NTUH-K2044 in response to iron availability. *Front. Cell Infect. Microbiol.* **2020**, *10*, 282. [[CrossRef](#)]
46. Huang, L.; Fu, L.; Hu, X.; Liang, X.; Gong, G.; Xie, C. Co-occurrence of *Klebsiella variicola* and *Klebsiella pneumoniae* both carrying bla (KPC) from a respiratory intensive care unit patient. *Infect. Drug Resist.* **2021**, *14*, 4503–4510. [[CrossRef](#)]
47. Cookson, A.L.; Biggs, P.J.; Marshall, J.C.; Reynolds, A.; Collis, R.M.; French, N.P. Culture independent analysis using *gnd* as a target gene to assess *Escherichia coli* diversity and community structure. *Sci. Rep.* **2017**, *7*, 841. [[CrossRef](#)]
48. Yang, X.B.; Wu, S.L.; Zhu, D.P.; Wu, H.; Jiang, T.; Qian, Y.H. Expression of the 2-dehydro-3-deoxyphosphooc-tonate aldolase (KdsA) gene in mulberry leaves (*Morus alba* L.) is down-regulated under high salt and drought stress. *Genet. Mol. Res.* **2015**, *14*, 11955–11964. [[CrossRef](#)]
49. Harvey, K.L.; Jarocki, V.M.; Charles, I.G.; Djordjevic, S.P. The diverse functional roles of elongation factor Tu (EF-Tu) in microbial pathogenesis. *Front. Microbiol.* **2019**, *10*, 2351. [[CrossRef](#)]
50. Niu, T.; Guo, L.; Luo, Q.; Zhou, K.; Yu, W.; Chen, Y. *Wza* gene knockout decreases *Acinetobacter baumannii* virulence and affects wzy-dependent capsular polysaccharide synthesis. *Virulence* **2020**, *11*, 1–13. [[CrossRef](#)]
51. De Luca, E.; Alvarez-Narvaez, S.; Maboni, G.; Baptista, R.P.; Nemeth, N.M.; Niedringhaus, K.D. Comparative genomics analyses support the reclassification of bisgaard taxon 40 as *Mergibacter* gen. nov., with *Mergibacter septicus* sp. nov. as type species: Novel insights into the phylogeny and virulence factors of a pasteurillaceae family member associated with mortality events in seabirds. *Front. Microbiol.* **2021**, *12*, 667356. [[CrossRef](#)] [[PubMed](#)]
52. Liu, Z.; Zhao, L.; Huang, L.; Qin, Y.; Zhang, J.; Zhang, J. Integration of RNA-seq and RNAi provides a novel insight into the immune responses of *Epinephelus coioides* to the *impB* gene of *Pseudomonas plecoglossicida*. *Fish Shellfish. Immunol.* **2020**, *105*, 135–143. [[CrossRef](#)] [[PubMed](#)]

53. Pira, H.; Risdian, C.; Musken, M.; Schupp, P.J.; Wink, J. *Photobacterium arenosum* WH24, isolated from the gill of pacific oyster *Crassostrea gigas* from the north sea of germany: Co-cultivation and prediction of virulence. *Curr. Microbiol.* **2022**, *79*, 219. [[CrossRef](#)] [[PubMed](#)]
54. Claret, L.; Miquel, S.; Vieille, N.; Ryjenkov, D.A.; Gomelsky, M.; Darfeuille-Michaud, A. The flagellar sigma factor *fliA* regulates adhesion and invasion of crohn disease-associated *Escherichia coli* via a cyclic dimeric GMP-dependent pathway. *J. Biol. Chem.* **2007**, *282*, 33275–33283. [[CrossRef](#)] [[PubMed](#)]
55. Araújo, B.F.; Ferreira, M.L.; Campos, P.A.; Royer, S.; Gonçalves, I.R.; da Fonseca Batistão, D.W. Hypervirulence and biofilm production in KPC-2-producing *Klebsiella pneumoniae* CG258 isolated in Brazil. *J. Med. Microbiol.* **2018**, *67*, 523–528. [[CrossRef](#)]
56. Jensen, S.O.; Reeves, P.R. Molecular evolution of the GDP-mannose pathway genes (*manB* and *manC*) in *Salmonella enterica*. *Microbiology-SGM* **2001**, *147 Pt 3*, 599–610. [[CrossRef](#)]
57. Wang, J.; Zhou, Z.; He, F.; Ruan, Z.; Jiang, Y.; Hua, X. The role of the type VI secretion system *vgrG* gene in the virulence and antimicrobial resistance of *Acinetobacter baumannii* ATCC 19606. *PLoS ONE* **2018**, *13*, e0192288. [[CrossRef](#)]
58. Barnell, W.O.; Liu, J.; Hesman, T.L.; O'Neill, M.C.; Conway, T. The zymomonas mobilis *glf*, *zwf*, *edd*, and *glk* genes form an operon: Localization of the promoter and identification of a conserved sequence in the regulatory region. *J. Bacteriol.* **1992**, *174*, 2816–2823. [[CrossRef](#)]
59. Planamente, S.; Salih, O.; Manoli, E.; Albesa-Jové, D.; Freemont, P.S.; Filloux, A. TssA forms a gp6-like ring attached to the type VI secretion sheath. *EMBO J.* **2016**, *35*, 1613–1627. [[CrossRef](#)]
60. Chen, Y.; Song, K.; Chen, X.; Li, Y.; Lv, R.; Zhang, Q. Attenuation of *Yersinia pestis fyuA* mutants caused by iron uptake inhibition and decreased survivability in macrophages. *Front. Cell. Infect. Microbiol.* **2022**, *12*, 874773. [[CrossRef](#)]
61. Magistro, G.; Magistro, C.; Stief, C.G.; Schubert, S. The high-pathogenicity island (HPI) promotes flagellum-mediated motility in extraintestinal pathogenic *Escherichia coli*. *PLoS ONE* **2017**, *12*, e0183950. [[CrossRef](#)] [[PubMed](#)]
62. Meneghetti, F.; Villa, S.; Gelain, A.; Barlocco, D.; Chiarelli, L.R.; Pasca, M.R. Iron acquisition pathways as targets for antitubercular drugs. *Curr. Med. Chem.* **2016**, *23*, 4009–4026. [[CrossRef](#)] [[PubMed](#)]
63. Tian, X.; Wang, Q.; Perlaza-Jimenez, L.; Zheng, X.; Zhao, Y.; Dhanasekaran, V. First description of antimicrobial resistance in carbapenem-susceptible *Klebsiella pneumoniae* after imipenem treatment, driven by outer membrane remodeling. *BMC Microbiol.* **2020**, *20*, 218. [[CrossRef](#)] [[PubMed](#)]
64. Bobrov, A.G.; Kirillina, O.; Fosso, M.Y.; Fetherston, J.D.; Miller, M.C.; VanCleave, T.T. Zinc transporters *YbtX* and *ZnuABC* are required for the virulence of *Yersinia pestis* in bubonic and pneumonic plague in mice. *Metallomics.* **2017**, *9*, 757–772. [[CrossRef](#)] [[PubMed](#)]
65. Arena, F.; Henrici De Angelis, L.; Pieralli, F.; Di Pilato, V.; Giani, T.; Torricelli, F. Draft genome sequence of the first hypermucoviscous *Klebsiella quasipneumoniae* subsp. *quasipneumoniae* isolate from a bloodstream infection. *Genome Announc.* **2015**, *3*, e00952-15. [[CrossRef](#)]
66. Besaury, L.; Bodilis, J.; Delgas, F.; Andrade, S.; De la Iglesia, R.; Ouddane, B. Abundance and diversity of copper resistance genes *cusA* and *copA* in microbial communities in relation to the impact of copper on Chilean marine sediments. *Mar. Pollut. Bull.* **2013**, *67*, 16–25. [[CrossRef](#)]
67. Shafer, C.M.; Tseng, A.; Allard, P.; McEvoy, M.M. Strength of Cu-efflux response in *Escherichia coli* coordinates metal resistance in *Caenorhabditis elegans* and contributes to the severity of environmental toxicity. *J. Biol. Chem.* **2021**, *297*, 101060. [[CrossRef](#)]
68. Zhen, Z.; Yan, C.; Zhao, Y. Influence of epiphytic bacteria on arsenic metabolism in *Hydrilla verticillata*. *Environ. Pollut.* **2020**, *261*, 114232. [[CrossRef](#)]
69. Bratu, S.; Landman, D.; George, A.; Salvani, J.; Quale, J. Correlation of the expression of *acrB* and the regulatory genes *marA*, *soxS* and *ramA* with antimicrobial resistance in clinical isolates of *Klebsiella pneumoniae* endemic to New York City. *J. Antimicrob. Chemother.* **2009**, *64*, 278–283. [[CrossRef](#)]
70. Hurtado-Escobar, G.A.; Grepinet, O.; Raymond, P.; Abed, N.; Velge, P.; Virlogeux-Payant, I. H-NS is the major repressor of *Salmonella Typhimurium* Pef fimbriae expression. *Virulence* **2019**, *10*, 849–867. [[CrossRef](#)]
71. Barroso, K.C.M.; Previato-Mello, M.; Batista, B.B.; Batista, J.H.; da Silva Neto, J.F. EmrR-dependent upregulation of the efflux pump *emrCAB* contributes to antibiotic resistance in *Chromobacterium violaceum*. *Front. Microbiol.* **2018**, *9*, 2756. [[CrossRef](#)] [[PubMed](#)]
72. Holden, E.R.; Webber, M.A. *MarA*, *ramA*, and *soxS* as mediators of the stress response: Survival at a cost. *Front. Microbiol.* **2020**, *11*, 828. [[CrossRef](#)] [[PubMed](#)]
73. Aiba, H. Autoregulation of the *Escherichia coli* *crp* gene: CRP is a transcriptional repressor for its own gene. *Cell* **1983**, *32*, 141–149. [[CrossRef](#)] [[PubMed](#)]
74. Monárrez, R.; Wang, Y.; Fu, Y.; Liao, C.H.; Okumura, R.; Braun, M.R. Genes and proteins involved in *qnrS1* induction. *Antimicrob. Agents Chemother.* **2018**, *62*, e00806-18. [[CrossRef](#)]
75. Furlan, J.P.R.; Lopes, R.; Gonzalez, I.H.L.; Ramos, P.L.; von Zeska Kress, M.R.; Stehling, E.G. Hypermucoviscous/hypervirulent and extensively drug-resistant *QnrB2*-, *QnrS1*-, and CTX-M-3-coproducing *Klebsiella pneumoniae* ST2121 isolated from an infected elephant (*Loxodonta africana*). *Vet. Microbiol.* **2020**, *251*, 108909. [[CrossRef](#)]
76. Srinivasan, V.B.; Rajamohan, G. *KpnEF*, a new member of the *Klebsiella pneumoniae* cell envelope stress response regulon, is an SMR-type efflux pump involved in broad-spectrum antimicrobial resistance. *Antimicrob. Agents Chemother.* **2013**, *57*, 4449–4462. [[CrossRef](#)]

77. Srinivasan, V.B.; Singh, B.B.; Priyadarshi, N.; Chauhan, N.K.; Rajamohan, G. Role of novel multidrug efflux pump involved in drug resistance in *Klebsiella pneumoniae*. *PLoS ONE* **2014**, *9*, e96288. [[CrossRef](#)]
78. Doménech-Sánchez, A.; Hernández-Allés, S.; Martínez-Martínez, L.; Benedí, V.J.; Albertí, S. Identification and characterization of a new porin gene of *Klebsiella pneumoniae*: Its role in beta-lactam antibiotic resistance. *J. Bacteriol.* **1999**, *181*, 2726–2732. [[CrossRef](#)]
79. Galetti, R.; Filho, R.; Ferreira, J.C.; Varani, A.M.; Sazinas, P.; Jelsbak, L. The plasmidome of multidrug-resistant emergent *Salmonella* serovars isolated from poultry. *Infect. Genet. Evol.* **2021**, *89*, 104716. [[CrossRef](#)]
80. Naha, S.; Sands, K.; Mukherjee, S.; Roy, C.; Rameez, M.J.; Saha, B. KPC-2-producing *Klebsiella pneumoniae* ST147 in a neonatal unit: Clonal isolates with differences in colistin susceptibility attributed to acrAB-TolC pump. *Int. J. Antimicrob. Agents.* **2020**, *55*, 105903. [[CrossRef](#)]
81. Ceccarelli, D.; Salvia, A.M.; Sami, J.; Cappuccinelli, P.; Colombo, M.M. New cluster of plasmid-located class 1 integrons in *Vibrio cholerae* O1 and a dfrA15 cassette-containing integron in *Vibrio parahaemolyticus* isolated in Angola. *Antimicrob. Agents. Chemother.* **2006**, *50*, 2493–2499. [[CrossRef](#)] [[PubMed](#)]
82. Hu, L.F.; Chen, G.S.; Kong, Q.X.; Gao, L.P.; Chen, X.; Ye, Y. Increase in the prevalence of resistance determinants to trimethoprim/sulfamethoxazole in clinical *Stenotrophomonas maltophilia* isolates in China. *PLoS ONE* **2016**, *11*, e0157693. [[CrossRef](#)] [[PubMed](#)]
83. Miryala, S.K.; Anbarasu, A.; Ramaiah, S. Role of SHV-11, a class A beta-lactamase, gene in multidrug resistance among *Klebsiella pneumoniae* strains and understanding Its mechanism by gene Network analysis. *Microb. Drug. Resist.* **2020**, *26*, 900–908. [[CrossRef](#)]
84. Dadashpour, R.; Moghaddam, M.J.M.; Salehi, Z. Prevalence of non-extended spectrum beta-lactamases SHV-1 and TEM-1 or -2 types in multidrug-resistant *Enterobacteriaceae* in northern Iran. *Biol. Futur.* **2020**, *71*, 419–426. [[CrossRef](#)] [[PubMed](#)]
85. Mondal, A.H.; Siddiqui, M.T.; Sultan, I.; Haq, Q.M.R. Prevalence and diversity of blaTEM, blaSHV and blaCTX-M variants among multidrug resistant *Klebsiella* spp. from an urban riverine environment in India. *Int. J. Environ. Health Res.* **2019**, *29*, 117–129. [[CrossRef](#)] [[PubMed](#)]
86. Fevre, C.; Passet, V.; Weill, F.X.; Grimont, P.A.; Brisse, S. Variants of the *Klebsiella pneumoniae* OKP chromosomal beta-lactamase are divided into two main groups, OKP-A and OKP-B. *Antimicrob. Agents Chemother.* **2005**, *49*, 5149–5152. [[CrossRef](#)] [[PubMed](#)]
87. Chen, Q.; Lu, W.; Zhou, D.; Zheng, G.; Liu, H.; Qian, C. Characterization of two macrolide resistance-related genes in multidrug-resistant *Pseudomonas aeruginosa* isolates. *Pol. J. Microbiol.* **2020**, *69*, 349–356. [[CrossRef](#)]
88. Chiu, H.C.; Lin, T.L.; Yang, J.C.; Wang, J.T. Synergistic effect of *imp/ostA* and *msbA* in hydrophobic drug resistance of *Helicobacter pylori*. *BMC Microbiol.* **2009**, *9*, 136. [[CrossRef](#)]
89. Lu, J.; Zhang, J.; Xu, L.; Liu, Y.; Li, P.; Zhu, T. Spread of the florfenicol resistance *floR* gene among clinical *Klebsiella pneumoniae* isolates in China. *Antimicrob. Resist. Infect. Control.* **2018**, *7*, 127. [[CrossRef](#)]
90. Breazeale, S.D.; Ribeiro, A.A.; Raetz, C.R. Oxidative decarboxylation of UDP-glucuronic acid in extracts of polymyxin-resistant *Escherichia coli*. origin of lipid a species modified with 4-amino-4-deoxy-L-arabinose. *J. Biol. Chem.* **2002**, *277*, 2886–2896. [[CrossRef](#)]
91. Jiang, S.S.; Lin, T.Y.; Wang, W.B.; Liu, M.C.; Hsueh, P.R.; Liaw, S.J. Characterization of UDP-glucose dehydrogenase and UDP-glucose pyrophosphorylase mutants of *Proteus mirabilis*: Defectiveness in polymyxin B resistance, swarming, and virulence. *Antimicrob. Agents Chemother.* **2010**, *54*, 2000–2009. [[CrossRef](#)] [[PubMed](#)]
92. Dwivedi, G.R.; Maurya, A.; Yadav, D.K.; Khan, F.; Gupta, M.K.; Gupta, P.; Darokar, M.P.; Srivastava, S.K. Comparative drug resistance reversal potential of natural glycosides: Potential of synergy niaziridin & niazirin. *Curr. Top. Med. Chem.* **2019**, *19*, 847–860. [[CrossRef](#)] [[PubMed](#)]
93. Fàbrega, A.; Martin, R.G.; Rosner, J.L.; Tavio, M.M.; Vila, J. Constitutive *soxS* expression in a fluoroquinolone-resistant strain with a truncated *soxR* protein and identification of a new member of the *marA-soxS-rob* regulon, *mdtG*. *Antimicrob. Agents Chemother.* **2010**, *54*, 1218–1225. [[CrossRef](#)]
94. Maunders, E.A.; Ganio, K.; Hayes, A.J.; Neville, S.L.; Davies, M.R.; Strugnell, R.A. The role of *zntA* in *Klebsiella pneumoniae* zinc homeostasis. *Microbiol. Spectr.* **2022**, *10*, e0177321. [[CrossRef](#)]
95. Chen, J.; Huang, L.; Wang, Q.; Zeng, H.; Xu, J.; Chen, Z. Antibiotics in aquaculture ponds from Guilin, south of China: Occurrence, distribution, and health risk assessment. *Environ. Res.* **2022**, *204*, 112084. [[CrossRef](#)] [[PubMed](#)]
96. Fatima, S.; Liaqat, F.; Akbar, A.; Sahfee, M.; Samad, A.; Anwar, M. Virulent and multidrug-resistant *Klebsiella pneumoniae* from clinical samples in Balochistan. *Int. Wound J.* **2021**, *18*, 510–518. [[CrossRef](#)]
97. Marques, C.; Menezes, J.; Belas, A.; Aboim, C.; Cavaco-Silva, P.; Trigueiro, G. *Klebsiella pneumoniae* causing urinary tract infections in companion animals and humans: Population structure, antimicrobial resistance and virulence genes. *J. Antimicrob. Chemother.* **2019**, *74*, 594–602. [[CrossRef](#)]
98. Varol, M.; Sunbul, M.R. Organochlorine pesticide, antibiotic and heavy metal residues in mussel, crayfish and fish species from a reservoir on the Euphrates River, Turkey. *Environ. Pollut.* **2017**, *230*, 311–319. [[CrossRef](#)]
99. Ni, L.; Chen, D.; Fu, H.; Xie, Q.; Lu, Y.; Wang, X.; Zhao, Y.; Chen, L. Residual levels of antimicrobial agents and heavy metals in 41 species of commonly consumed aquatic products in Shanghai, China, and cumulative exposure risk to children and teenagers. *Food Control.* **2021**, *129*, 108225. [[CrossRef](#)]
100. Yu, X.; Zhang, W.; Zhao, Z.; Ye, C.; Zhou, S.; Wu, S. Molecular characterization of carbapenem-resistant *Klebsiella pneumoniae* isolates with focus on antimicrobial resistance. *BMC Genom.* **2019**, *20*, 822. [[CrossRef](#)]

101. Fortier, L.C.; Sekulovic, O. Importance of prophages to evolution and virulence of bacterial pathogens. *Virulence* **2013**, *4*, 354–365. [[CrossRef](#)] [[PubMed](#)]
102. Bleriot, I.; Trastoy, R.; Blasco, L.; Fernandez-Cuenca, F.; Ambroa, A.; Fernandez-Garcia, L. Genomic analysis of 40 prophages located in the genomes of 16 carbapenemase-producing clinical strains of *Klebsiella pneumoniae*. *Microb. Genom.* **2020**, *6*, e000369. [[CrossRef](#)] [[PubMed](#)]
103. Gillings, M.; Boucher, Y.; Labbate, M.; Holmes, A.; Krishnan, S.; Holley, M. The evolution of class 1 integrons and the rise of antibiotic resistance. *J. Bacteriol.* **2008**, *190*, 5095–5100. [[CrossRef](#)] [[PubMed](#)]
104. Firoozeh, F.; Mahluji, Z.; Khorshidi, A.; Zibaei, M. Molecular characterization of class 1, 2 and 3 integrons in clinical multi-drug resistant *Klebsiella pneumoniae* isolates. *Antimicrob. Resist. Infect. Control.* **2019**, *8*, 59. [[CrossRef](#)]
105. Nzabarushimana, E.; Tang, H. Insertion sequence elements-mediated structural variations in bacterial genomes. *Mob. DNA* **2018**, *9*, 29. [[CrossRef](#)]
106. Devi, V.; Harjai, K.; Chhibber, S. CRISPR-Cas systems: Role in cellular processes beyond adaptive immunity. *Folia. Microbiol.* **2022**, *67*, 837–850. [[CrossRef](#)]
107. Wu, Y.; Battalapalli, D.; Hakeem, M.J.; Selamneni, V.; Zhang, P.; Draz, M.S. Engineered CRISPR-Cas systems for the detection and control of antibiotic-resistant infections. *J. Nanobiotechnol.* **2021**, *19*, 401. [[CrossRef](#)]
108. Remya, P.A.; Shanthi, M.; Sekar, U. Characterisation of virulence genes associated with pathogenicity in *Klebsiella pneumoniae*. *Indian J. Med. Microbiol.* **2019**, *37*, 210–218. [[CrossRef](#)]
109. Kuş, H.; Arslan, U.; Türk Dağı, H.; Findık, D. Investigation of various virulence factors of *Klebsiella pneumoniae* strains isolated from nosocomial infections. *Mikrobiyol. Bul.* **2017**, *51*, 329–339. [[CrossRef](#)]
110. van Duin, D.; Paterson, D.L. Multidrug-resistant bacteria in the community: An update. *Infect. Dis. Clin. N. Am.* **2020**, *34*, 709–722. [[CrossRef](#)]
111. Tan, T.Y.; Ong, M.; Cheng, Y.; Ng, L.S.Y. Hypermucoviscosity, *rmpA*, and *aerobactin* are associated with community-acquired *Klebsiella pneumoniae* bacteremic isolates causing liver abscess in Singapore. *J. Microbiol. Immunol. Infect.* **2019**, *52*, 30–34. [[CrossRef](#)] [[PubMed](#)]
112. Candan, E.D.; Aksoz, N. *Klebsiella pneumoniae*: Characteristics of carbapenem resistance and virulence factors. *Acta. Biochim. Pol.* **2015**, *62*, 867–874. [[CrossRef](#)] [[PubMed](#)]
113. Ssekatawa, K.; Byarugaba, D.K.; Nakavuma, J.L.; Kato, C.D.; Ejobi, F.; Tweyongyere, R.; Eddie, W.M. Prevalence of pathogenic *Klebsiella pneumoniae* based on PCR capsular typing harbouring carbapenemases encoding genes in Uganda tertiary hospitals. *Antimicrob. Resist. Infect. Control.* **2021**, *10*, 57. [[CrossRef](#)] [[PubMed](#)]

Disclaimer/Publisher’s Note: The statements, opinions and data contained in all publications are solely those of the individual author(s) and contributor(s) and not of MDPI and/or the editor(s). MDPI and/or the editor(s) disclaim responsibility for any injury to people or property resulting from any ideas, methods, instructions or products referred to in the content.